Bulk viscosity, particle spectra, and flow in heavy-ion collisions

Kevin Dusling and Thomas Schäfer
Department of Physics, North Carolina State University, Raleigh, North Carolina 27695, USA
(Received 21 October 2011; revised manuscript received 11 January 2012; published 9 April 2012)

We study the effects of bulk viscosity on p_T spectra and elliptic flow in heavy-ion collisions. For this purpose, we compute the dissipative correction δf to the single-particle distribution functions in leading-log QCD, and in several simplified models. We consider, in particular, the relaxation time approximation and a kinetic model for the hadron resonance gas. We implement these distribution functions in a hydrodynamic simulation of Au + Au collisions at the Relativistic Heavy Ion Collider (RHIC). We find significant corrections due to bulk viscosity in hadron p_T spectra and the differential elliptic flow parameter $v_2(p_T)$. We observe that bulk viscosity scales as the second power of conformality breaking $\zeta \sim \eta(c_s^2 - 1/3)^2$, whereas δf scales as the first power. Corrections to the spectra are therefore dominated by viscous corrections to the distribution function, and reliable bounds on the bulk viscosity require accurate calculations of δf in the hadronic resonance phase. Based on viscous hydrodynamic simulations and a simple kinetic model of the resonance phase, which correctly extrapolates to the kinetic description of a dilute pion gas, we conclude that it is difficult to describe the v_2 spectra at RHIC unless $\zeta/s \lesssim 0.05$ near freeze-out. We also find that effects of the bulk viscosity on the p_T integrated v_2 are small.

DOI: 10.1103/PhysRevC.85.044909 PACS number(s): 25.75.−q

I. INTRODUCTION

One of the fascinating discoveries of the Relativistic Heavy Ion Collider (RHIC) program is the near ideal nature of the fluid produced in the collision of two heavy nuclei [1–5]. There is a general consensus in the community that the ratio of the shear viscosity to the entropy density of the system is no more than a few times the bound $\eta/s \gtrsim 1/4\pi$ conjectured by Kovtun, Son, and Starinets [6]. However, it is difficult to determine the level of accuracy that can be obtained when extracting the transport properties. To date, the best estimate of the shear viscosity comes from a detailed comparison of particle spectra and elliptic flow with viscous hydrodynamic simulations [7]. But, within these state-of-the-art calculations, there are many systematic uncertainties which are not fully under control. Some of these include the precise form of the initial condition, the details of the equation of state, the handling of the freeze-out dynamics, and the role of bulk viscosity. Irrespective of its role in constraining shear viscosity, the bulk viscosity of the matter produced at RHIC and the Large Hadron Collider (LHC) is clearly an interesting quantity in itself. In this work, we will study the effects of bulk viscosity on the spectra and the elliptic flow parameter. Our goal is to assess the uncertainty in the extraction of η/s due to the bulk viscosity, and to identify observables that constrain the bulk viscosity.

The earliest viscous hydrodynamic simulations only included corrections due to shear viscosity. One could argue that this may be a safe assumption as there are a number of physical systems, possibly relevant to heavy-ion collisions, where the bulk viscosity is zero or negligible. For example, it is well known that bulk viscosity vanishes in both the nonrelativistic and ultrarelativistic limits of a gas when the number of particles are conserved [10]. In a weakly coupled quark-gluon plasma, it was found that the bulk viscosity is on the order of 1000 times smaller than the shear viscosity [11]. Finally, in the simplest kinetic model, the relaxation time approximation, one finds that the bulk viscosity goes as the square of the deviation from conformality,

$$\zeta \approx 15\eta\left(\tfrac{1}{3} - c_s^2\right)^2. \tag{1}$$

The above relation was first found by Weinberg for a photon gas coupled to matter [12]. It also happens to give parametrically correct results for weakly coupled QCD, but not for a scalar field theory. In the context of AdS/CFT, an analogous relationship [13] has been found:

$$\zeta \gtrsim 2\eta\left(\tfrac{1}{3} - c_s^2\right). \tag{2}$$

In this case, the bulk viscosity is proportional to the first power of conformal breaking. Based on these above examples, it is clear that for a system which is nearly conformally invariant (such as weakly coupled QCD), the bulk viscosity will be small. However, lattice QCD computations [14] have shown that the equation of state differs strongly from the conformal limit at temperatures relevant to heavy-ion collisions (see Fig. 1). For example, if the speed of sound approaches $c_s^2 \approx 0.2$ near the phase transition, we find $\zeta \approx 0.25\eta$ using either of the expressions (1) or (2) given above. Even larger values $\zeta \approx 0.6\eta$ have been obtained in direct lattice studies of the bulk viscosity in the regime $T = (1.25\text{–}1.65)T_c$ [15]. It is therefore important to study how bulk viscosity modifies hadronic observables, such as p_T spectra and elliptic flow. Previous studies of this type can be found in [16–23].

We begin by reminding the reader how shear viscosity manifests itself in the spectra of produced particles. The equation of hydrodynamics expresses the conservation of the energy momentum tensor

$$\partial_\mu T^{\mu\nu} = 0, \tag{3}$$

which is given as a sum of ideal and dissipative parts,

$$T^{\mu\nu} = (\epsilon + \mathcal{P})u^\mu u^\nu + \mathcal{P}g^{\mu\nu} + \pi^{\mu\nu} + \Pi\Delta^{\mu\nu}. \tag{4}$$

In the above expression for the stress-energy tensor, we have used the definition of the three-frame projector $\Delta^{\mu\nu} = g^{\mu\nu} +$

 ©2012 American Physical Society

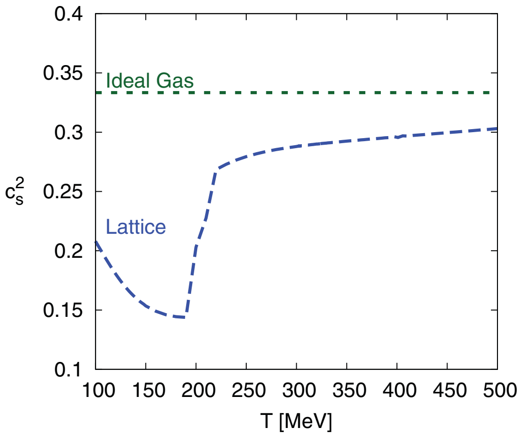

FIG. 1. (Color online) Sound speed squared as a function of temperature from the parametrization of the lattice QCD equation of state given in [8]. See [9] for a discussion of the various parametrizations available for the QCD equation of state.

$u^\mu u^\nu$. In the first-order (or Navier-Stokes) approximation, the dissipative parts of the stress-energy tensor can be written in the local rest frame as

$$\pi^{ij} = -\eta\left(\partial^i u^j + \partial^j u^i - \tfrac{2}{3}\delta^{ij}\partial_k u^k\right) = -\eta\sigma^{ij} \equiv -2\eta\langle\partial^i u^j\rangle, \tag{5}$$

$$\Pi = -\zeta\,\partial_k u^k, \tag{6}$$

where η (ζ) is the shear (bulk) viscosity and $\langle\cdots\rangle$ indicates that the bracketed tensor should be symmetrized and made traceless. In principle, it would be satisfactory to solve the relativistic Navier-Stokes equations in order to compute the first-order viscous correction to particle spectra. However, the first-order theory is plagued with difficulties such as instabilities and violations of causality. In order to circumvent these difficulties, it is necessary to use a second-order theory, such as the one proposed by Israel and Stewart [24,25] or Öttinger and Grmela [26,27]. The two theories are qualitatively the same in that they both approach the first-order theory for small relaxation times. In this work, we will not be interested in the higher-order corrections arising from the second-order theory. Instead, we use second-order hydrodynamics as a practical way to obtain the lowest-order correction in going from ideal to Navier-Stokes hydrodynamics.

The solution to the Navier-Stokes equations will lead to viscous corrections to the resulting temperature and flow profiles. Particle spectra are then computed using the Cooper-Frye [28] formula

$$E_{\mathbf{p}}\frac{dN}{d^3p} = \frac{1}{(2\pi)^3}\int_\sigma f(E_{\mathbf{p}})p^\mu d\sigma_\mu, \tag{7}$$

where σ_μ is the freeze-out hypersurface taken as a surface of constant energy density in this work. For a system out of equilibrium, $f(E_{\mathbf{p}})$ is not the equilibrium distribution function but also contains viscous corrections

$$f(E_{\mathbf{p}}) = f_0(E_{\mathbf{p}}) + \delta f(E_{\mathbf{p}}), \tag{8}$$

where f_0 is the usual equilibrium Bose-Fermi distribution function. The only constraint on δf is that the stress-energy tensor remains continuous across the freeze-out hypersurface:

$$\delta T^{\mu\nu} = \int \frac{d^3\mathbf{p}}{(2\pi)^3 E_{\mathbf{p}}} p^\mu p^\nu \delta f(E_{\mathbf{p}}). \tag{9}$$

As shown in [29], this constraint still leaves a lot of freedom in the form of δf for shear viscosity. It was argued that the functional form of δf could fall anywhere between a linearly increasing function of momentum to a quadratically increasing function of momentum. These two forms of the distribution function lead to qualitatively different behavior for $v_2(p_T)$ as demonstrated by the right plot of Fig. 2. By definition, $v_2(p_T)$ is given by

$$v_2(p_T) \equiv \frac{\int d\phi\cos(2\phi)\,(dN + \delta dN)}{\int d\phi\,(dN + \delta dN)}, \tag{10}$$

where dN is short for $dN/(dp_T\,d\phi)$ and δdN is the first viscous correction to this. If, as a pedagogical exercise we neglect the viscous correction to the distribution function all together (which violates energy-momentum conservation across the freeze-out surface), $v_2(p_T)$ would follow the curve labeled "f_0" as shown in the left plot of Fig. 2. Clearly, the form of the viscous correction to the distribution function will play an important role in extracting the shear viscosity.

There is an analogous viscous correction to the distribution function coming from bulk viscosity as well. The main goal of this work is to characterize the functional form of δf due to bulk viscosity for various theories and models. We will also show how bulk viscous corrections exhibit themselves in spectra as well as some phenomenological consequences.

II. BOLTZMANN TRANSPORT EQUATION

Let us first start by setting up the notation that will be used throughout this work. The equilibrium distribution functions for bosons and fermions are

$$n_{\mathbf{p}} = \frac{1}{e^{\beta E_{\mathbf{p}}} \mp 1}, \tag{11}$$

where the upper (minus) sign is for bosons and the lower (plus) sign is for fermions. We will use capital letters P, Q to label 4-vectors and bold type $\mathbf{p}$, $\mathbf{q}$ for their corresponding 3-vector components having energy $E_{\mathbf{p}}, E_{\mathbf{q}}$. The magnitude of the three-momentum will be written as p, q. The sign convention for the metric tensor is $[-,+,+,+]$ and therefore the hydrodynamic fluid four-velocity obeys the normalization condition $u_\mu u^\mu = -1$. We also use the notation $\omega_{\mathbf{p}} \equiv P_\mu(\beta)u^\mu(t,\mathbf{x})$ for the quasiparticle's energy in the laboratory frame having four-momentum $P^\mu = (P^0 \equiv E_{\mathbf{p}}, \mathbf{p})$ in the local rest frame.

The starting point for our analysis will always be the Boltzmann transport equation

$$\mathcal{D}f(t,\mathbf{x},\mathbf{p}) \equiv (\partial_t + v_{\mathbf{p}}\cdot\partial_{\mathbf{x}} + \mathbf{F}\cdot\partial_{\mathbf{p}})f(t,\mathbf{x},\mathbf{p}) = -\mathcal{C}[f,\mathbf{p}], \tag{12}$$

where $v_{\mathbf{p}}$ is the particle's velocity and $\mathbf{F}$ is the external force on the particle,

$$v_{\mathbf{p}} \equiv \partial_{\mathbf{p}}E_{\mathbf{p}}\,, \qquad \mathbf{F} \equiv \frac{d\mathbf{p}}{dt} = -\partial_{\mathbf{x}}E_{\mathbf{p}}. \tag{13}$$

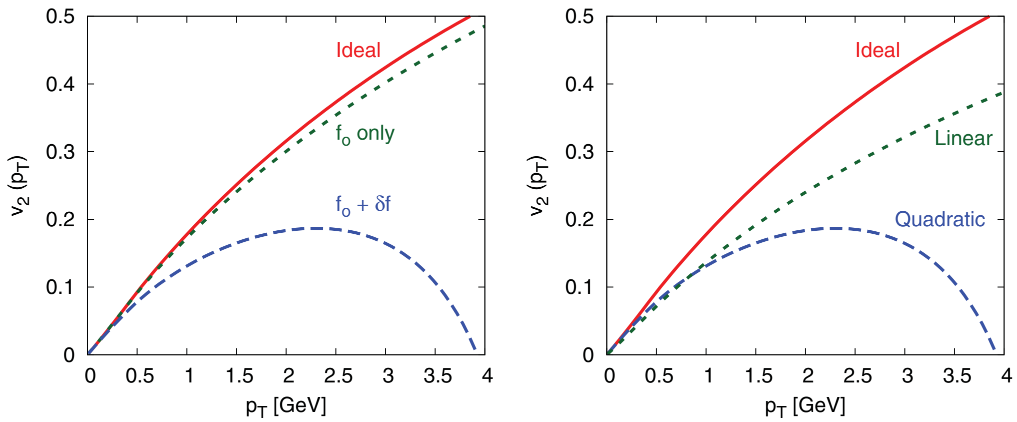

FIG. 2. (Color online) Typical results for $v_2(p_T)$ from a viscous hydrodynamic model using a quadratic deviation from equilibrium; $\delta f(\mathbf{p}) \sim p^2$. The left plot also shows the viscous result without including the off-equilibrium correction to the distribution function. The right plot compares the quadratic ansatz with a linear ansatz; $\delta f(\mathbf{p}) \sim p$. Both curves result in the same shear viscosity to entropy ratio.

In this work, we will consider only small deviations from local thermal equilibrium and therefore expand the Boltzmann equation around the local thermal equilibrium solution

$$f\text{eq}(t, \mathbf{x}, \mathbf{p}) = \frac{1}{e^{-\beta(t,\mathbf{x})\omega_{\mathbf{p}}(t,\mathbf{x})} \mp 1}. \tag{14}$$

This procedure is known as the Chapman-Enskog expansion. In the Chapman-Enskog procedure, we expand the left-hand side of the Boltzmann equation in gradients of the thermodynamic variables and linearize the collision operator in $\delta f = f - f\text{eq}$. Using the relations[1]

$$\frac{\partial f\text{eq}}{\partial \beta} = n_{\mathbf{p}}(1 \pm n_{\mathbf{p}})\frac{\partial(\beta\omega_{\mathbf{p}})}{\partial\beta}, \tag{15}$$

$$\frac{\partial f\text{eq}}{\partial \omega_{\mathbf{p}}} = n_{\mathbf{p}}(1 \pm n_{\mathbf{p}})\beta, \tag{16}$$

the left-hand side of the Boltzmann equation can be written as[2]

$$\frac{\mathcal{D} f\text{eq}}{n_{\mathbf{p}}(1 \pm n_{\mathbf{p}})} = \frac{\partial(\beta E_{\mathbf{p}})}{\partial\beta}(\partial_t + v_{\mathbf{p}} \cdot \partial_{\mathbf{x}})\beta + \beta(\partial_t + v_{\mathbf{p}} \cdot \partial_{\mathbf{x}} + \mathbf{F} \cdot \partial_{\mathbf{p}})\omega_{\mathbf{p}}. \tag{17}$$

Let us now assume that the quasiparticles in our system have a dispersion relation of the form

$$E_{\mathbf{p}} = \sqrt{m^2(\beta(\mathbf{x}, t)) + \mathbf{p}^2}, \tag{18}$$

where we have implicitly included a mass that may be a function of temperature. With this dispersion relation, the following identities hold:

$$v_{\mathbf{p}} = \frac{\mathbf{p}}{E_{\mathbf{p}}}, \qquad \mathbf{F} = -\frac{m}{E_{\mathbf{p}}}\partial_{\mathbf{x}} m = -\frac{\partial E_{\mathbf{p}}}{\partial\beta}\partial_{\mathbf{x}}\beta. \tag{19}$$

Making use of the above relations, the left-hand side of the Boltzmann equation can be rewritten as[3]

$$\frac{E_{\mathbf{p}}\mathcal{D} f_{\text{eq}}}{\beta n_{\mathbf{p}}(1 \pm n_{\mathbf{p}})} = \frac{1}{2}p^i p^j \sigma_{ij} + \partial_i u^i\left(\frac{p^2}{3} - c_s^2 E_{\mathbf{p}}\frac{\partial(\beta E_{\mathbf{p}})}{\partial\beta}\right), \tag{20}$$

where we have defined

$$\sigma^{ij} = 2\langle\partial^i u^j\rangle = \left(\partial^i u^j + \partial^j u^i - \tfrac{2}{3}\delta^{ij}\partial_k u^k\right). \tag{21}$$

In order to match the kinetic description to hydrodynamics, we need to define a covariantly conserved energy-momentum tensor in the kinetic theory. There is a subtlety that comes about due to the space-time dependence of the mass in the dispersion relation. In order to see this, let us first start with the canonical form of the stress-energy tensor, which is typically used in kinetic theory

$$T^{\mu\nu}(t, \mathbf{x}) = \int \frac{d^3\mathbf{p}}{(2\pi)^3 E_{\mathbf{p}}} P^\mu P^\nu f(t, \mathbf{x}, \mathbf{p}). \tag{22}$$

For situations where the dispersion relation is independent of the medium, this form is satisfactory as one can show that energy and momentum is covariantly conserved.[4] Here,

$$\partial_\mu T^{\mu\nu} = 0. \tag{25}$$

In the case where we have a nontrivial dispersion relation, the partial integration can not pass through the integration

[1]Two useful identities are $\partial n_{\mathbf{p}}/\partial p = -n_{\mathbf{p}}(1 \pm n_{\mathbf{p}})$ and $\partial^2 n_{\mathbf{p}}/\partial p^2 = n_{\mathbf{p}}(1 \pm n_{\mathbf{p}})(1 \pm 2n_{\mathbf{p}})$.

[2]Even though we are working in the local rest frame, gradients that are acting on the flow velocity are still nonvanishing. For example, $\partial_\mu u^i \neq 0$ but $\partial_\mu u^0 = 0$ since $u_\mu u^\mu = -1$.

[3]In deriving this expression, we have used the two equilibrium identities $\partial_t u_i = \partial_i \ln\beta$ and $\partial_t \ln\beta = c_s^2 \partial_i u^i$.

[4]This can be seen by using the definition of the stress-energy tensor given in Eq. (22) and differentiating both sides. For the specific case where the dispersion relation is independent of space-time, we find

$$\partial_\mu T^{\mu\nu} = \int \frac{d^3\mathbf{p}}{(2\pi)^3 E_{\mathbf{p}}} p^\nu p^\mu \partial_\mu f(t, \mathbf{x}, \mathbf{p}). \tag{23}$$

measure. Instead, we find that

$$\partial_\mu T^{\mu\nu} = S^\nu, \tag{26}$$

where

$$S^\nu = \int \frac{d^3\mathbf{p}}{(2\pi)^3} f(t,\mathbf{x},\mathbf{p})\partial_\mu\left(\frac{P^\mu P^\nu}{E_\mathbf{p}}\right) - \int \frac{d^3\mathbf{p}}{(2\pi)^3} P^\nu\, \mathbf{F}\cdot\partial_\mathbf{p} f(t,\mathbf{x},\mathbf{p}). \tag{27}$$

We would like to modify the stress-energy tensor such that the above source term vanishes. This can be achieved by using the definition

$$T^{\mu\nu} = \int \frac{d^3\mathbf{p}}{(2\pi)^3 E_\mathbf{p}}\left(P^\mu P^\nu - u^\mu u^\nu T^2\frac{\partial m^2}{\partial T^2}\right) f(t,\mathbf{x},\mathbf{p}). \tag{28}$$

Throughout this work, we will always use this modified form of the stress-energy tensor when matching from the kinetic theory to the macroscopic hydrodynamic fields. We stress that if the quasiparticle's mass is space-time independent, the above two definitions of the stress-energy tensor coincide. We also note that these observations are not new. The modified form of the stress-energy tensor was used in studies of the bulk viscosity of a hadronic gas [30–33] and of scalar field theory [34,35].

III. RELAXATION TIME APPROXIMATION

In this section, we consider the simplest form of the collision kernel, which is known as the relaxation time approximation (RTA) or Bhatnagar-Gross-Krook (BGK) approximation. In this model, the collision term has the simple form

$$\mathcal{C}[f,\mathbf{p}] = \frac{f(\mathbf{p}) - n_\mathbf{p}}{\tau_R(E_\mathbf{p})}. \tag{29}$$

If we define the deviation from equilibrium as $\delta f(t,\mathbf{x},\mathbf{p}) \equiv n_p - f(\mathbf{p})$ and use the linearized form of the streaming operator given in Eq. (20), we find that

$$\delta f = -\frac{\tau_R(E_\mathbf{p})}{E_\mathbf{p} T} n_\mathbf{p}(1\pm n_\mathbf{p}) \times \left[\frac{1}{2}p^i p^j \sigma_{ij} + \partial_i u^i\left(\frac{p^2}{3} - c_s^2 E_\mathbf{p}\frac{\partial(\beta E_\mathbf{p})}{\partial\beta}\right)\right]. \tag{30}$$

We would now like to identify the relaxation time encoded in δf with the transport coefficients η and ζ. First, we start with the shear viscosity. Looking at any of the off-diagonal components of the stress-energy tensor given in Eqs. (4) and (28), we find in the local rest frame

$$\delta T^{xy} = -2\eta\langle\partial^x u^y\rangle = \int \frac{d^3\mathbf{p}}{(2\pi)^3}\frac{p^x p^y}{E_\mathbf{p}}\delta f, \tag{31}$$

and the shear viscosity can be identified as

$$\eta = \frac{\beta}{30\pi^2}\int \frac{p^6}{E_\mathbf{p}^2}\tau_R(E_\mathbf{p}) n_\mathbf{p}(1\pm n_\mathbf{p})\, dp. \tag{32}$$

If we take a relaxation time of the form[5]

$$\tau_R(E_\mathbf{p}) = \tau_0\beta(\beta E_\mathbf{p})^{1-\alpha}, \tag{33}$$

we find the following relation between the shear viscosity and relaxation time:

$$\eta = \frac{\tau_0 T^3}{30\pi^2}\mathcal{I}_\alpha(\beta m), \tag{34}$$

where the dimensionless phase-space integral $\mathcal{I}_\alpha$ is worked out in Appendix B1.

We now come to bulk viscosity, which characterizes the deviation of the pressure from its equilibrium value as the fluid expands or contracts more quickly than the time it takes the pressure to relax back to its equilibrium value. The bulk viscous pressure Π is therefore related to the extra pressure from the departure from equilibrium δf. However, the departure from equilibrium can not only shift the pressure but also the energy density by an amount $\delta\epsilon$. This shift in energy density will also lead to a shift in pressure, which should not be included in the bulk viscous pressure. This is because the bulk viscous pressure should only include the difference between the actual pressure and the pressure determined by thermodynamics [11], which in our case will be $\mathcal{P}(\epsilon+\delta\epsilon)$. This additional pressure shift must therefore be subtracted when defining the bulk viscous pressure[6]

$$\Pi \equiv \frac{1}{3}T^{ii} - \mathcal{P}(\epsilon+\delta\epsilon) = \int \frac{d^3\mathbf{p}}{(2\pi)^3 E_\mathbf{p}}\left(\frac{p^2}{3} - c_s^2 E_\mathbf{p}\frac{\partial(\beta E_\mathbf{p})}{\partial\beta}\right)\delta f. \tag{37}$$

By making use of the form of the dispersion relation in Eq. (18), it will be convenient to define the quantities $\tilde{m}$ and $\tilde{E}_\mathbf{p}$ via

$$E_\mathbf{p}\frac{\partial(\beta E_\mathbf{p})}{\partial\beta} = p^2 + \left(m^2 - \frac{\partial m^2}{\partial T^2}T^2\right) \equiv p^2 + \tilde{m}^2 \equiv \tilde{E}_\mathbf{p}^2. \tag{38}$$

In this case, the Boltzmann equation is $p^\mu\partial_\mu f(t,\mathbf{x},\mathbf{p}) = -E_\mathbf{p}\mathcal{C}[f,\mathbf{p}]$ and we find

$$\partial_\mu T^{\mu\nu} = -\int \frac{d^3\mathbf{p}}{(2\pi)^3} p^\nu \mathcal{C}[f,\mathbf{p}]. \tag{24}$$

The four-momentum is a collisional invariant and the right-hand side vanishes.

[5]We follow the notation of [29] whereby taking $\alpha = 0$ corresponds to the usual quadratic ansatz. In this case, the relaxation time grows linearly with momentum $\tau_R \sim E_\mathbf{p}$ and $\chi \sim p^2$. The other extreme case follows from $\alpha = 1$ where now the relaxation is independent of momentum, $\tau_R \sim$ const and $\chi \sim p$. For leading-order QCD, one numerically finds $\alpha = 0.62$ and $\chi \sim p^{1.38}$.

[6]We have used

$$\mathcal{P}(\epsilon_0+\delta\epsilon) \approx \mathcal{P}(\epsilon_0) + c_s^2\delta e, \tag{35}$$

where from Eq. (28) we have

$$\delta\epsilon = \int \frac{d^3\mathbf{p}}{(2\pi)^3 E_\mathbf{p}}\left(E_\mathbf{p}^2 - T^2\frac{\partial m^2}{\partial T^2}\right)\delta f. \tag{36}$$

The following relation between the relaxation time and bulk viscosity coefficient ζ then holds:

$$\zeta = \frac{\tau_0 T^3}{2\pi^2}\mathcal{J}_\alpha(\beta m, \beta\tilde{m}), \tag{39}$$

where the dimensionless phase-space integral $\mathcal{J}_\alpha$ depends on both the thermal mass m and the shifted mass $\tilde{m}$. This phase-space integral is discussed at length in Appendix B1. In the high-temperature limit ($T \gg m, \tilde{m}$), one finds

$$\eta = \frac{\tau_0 T^3}{30\pi^2}\overline{\Gamma}(6-\alpha), \qquad \zeta = \frac{\tau_0 T^3}{2\pi^2}\overline{\Gamma}(6-\alpha)\left(\frac{1}{3}-c_s^2\right)^2, \tag{40}$$

where the function $\overline{\Gamma}$, defined in Appendix B1, depends on the statistics of the particles. For classical statistics, $\overline{\Gamma}$ is the usual gamma function. From the above formulas, we can recover the well-known relationship [36] between shear and bulk viscosity,

$$\zeta = 15\eta\left(\tfrac{1}{3}-c_s^2\right)^2. \tag{41}$$

We note that this relation is independent of the momentum dependence of the relaxation time.

A. Landau matching in the relaxation time approximation

Landau matching is a way to uniquely specify the energy density ϵ and fluid four-velocity u^μ in terms of four-components of $T^{\mu\nu}$. If we use the Landau-Lifshitz convention

$$\epsilon = u_\mu u_\nu T^{\mu\nu}, \tag{42}$$

$$\epsilon u^\mu = -u_\nu T^{\mu\nu}, \tag{43}$$

then the other six independent components of $T^{\mu\nu}$ are given by a nonequilibrium stress tensor $\pi^{\mu\nu}$ satisfying $u_\mu\pi^{\mu\nu}=0$. In order that the stress-energy tensor remains continuous across the freeze-out surface, the functional form of δf must be such that the Landau-matching condition is satisfied; $u_\mu\delta T^{\mu\nu}=0$. From Eq. (28), the matching condition is

$$0 = \int \frac{d^3\mathbf{p}}{(2\pi)^3 E_\mathbf{p}}\left(\omega_\mathbf{p} P^\nu + u^\nu T^2\frac{\partial m^2}{\partial T^2}\right)\delta f(E_\mathbf{p}). \tag{44}$$

It is sufficient for the above matching condition to be satisfied in the local rest frame. This corresponds to the condition that the shift in energy density stemming from δf vanishes:

$$\delta\epsilon = 0 = \int \frac{d^3\mathbf{p}}{(2\pi)^3 E_\mathbf{p}}\tilde{E}_\mathbf{p}^2\,\delta f(E_\mathbf{p}). \tag{45}$$

Let us now look at the energy density shift coming from the off-equilibrium distribution given in Eq. (30):

$$\delta\epsilon_{\rm RTA} = \frac{\Pi\beta^5}{\mathcal{J}_\alpha(\beta m,\beta\tilde{m})}\int\frac{d^3\mathbf{p}}{(2\pi)^3}\left(\frac{\tilde{E}_\mathbf{p}}{E_\mathbf{p}}\right)^2 n_\mathbf{p}(1\pm n_\mathbf{p}) \times\left(\frac{p^2}{3}-c_s^2\tilde{E}_\mathbf{p}^2\right)(\beta E_\mathbf{p})^{1-\alpha}. \tag{46}$$

The above expression simplifies considerably when there are no mean fields $\tilde{E}_\mathbf{p}\to E_\mathbf{p}$:

$$\delta\epsilon_{\rm RTA} \propto \int\frac{d^3\mathbf{p}}{(2\pi)^3}n_\mathbf{p}(1\pm n_\mathbf{p})\left(\frac{p^2}{3}-c_s^2E_\mathbf{p}^2\right)(\beta E_\mathbf{p})^{1-\alpha}. \tag{47}$$

The above integral vanishes only for $\alpha=1$, which is the case where the relaxation time $\tau_R(E_\mathbf{p})$ is momentum independent.[7] Therefore, if one considers a gas of particles where the deviation from conformality comes from the bare mass of the particle only (no mean fields), then the relaxation time approximation can be used if and only if the relaxation time is independent of momentum.

In the presence of mean fields (i.e., the quasiparticle's mass is temperature dependent), we can write Eq. (46) as

$$\delta\epsilon_{\rm RTA} \propto \int\frac{d^3\mathbf{p}}{(2\pi)^3}n_\mathbf{p}(1\pm n_\mathbf{p})\left(\frac{p^2}{3}-c_s^2\tilde{E}_\mathbf{p}^2\right)(\beta E_\mathbf{p})^{1-\alpha} - \frac{\partial m^2}{\partial T^2}\int\frac{d^3\mathbf{p}}{(2\pi)^3}n_\mathbf{p}(1\pm n_\mathbf{p}) \times\left(\frac{p^2}{3}-c_s^2\tilde{E}_\mathbf{p}^2\right)(\beta E_\mathbf{p})^{-\alpha-1}. \tag{49}$$

In this case, taking $\alpha=1$ makes the first term vanish, but the second term remains finite (even though it may be parametrically small since it is proportional to the coupling). It is possible, however, to use the relaxation time approximation consistent with Landau matching by a fine tuning of the parameter α.

IV. SCALAR FIELD THEORY

The case of a weakly coupled scalar field theory was studied by Jeon [34], where the Boltzmann equation and collision kernel were derived from first principles. While the full computation of the transport coefficients are numerically intensive, a lot can be said about the form of the off-equilibrium distribution function from certain general considerations. As shown in [35], one can compute the transport coefficients in $g\phi^3+\lambda\phi^4$ theory at weak coupling by solving Boltzmann equation[8]

$$(\partial_t + v_\mathbf{p}\cdot\partial_\mathbf{x} + \mathbf{F}\cdot\partial_\mathbf{p})f(t,\mathbf{x},\mathbf{p}) = -\mathcal{C}_{2\leftrightarrow 2}[f,\mathbf{p}] - \mathcal{C}_{2\leftrightarrow 4}[f,\mathbf{p}], \tag{50}$$

where the collision operator has been split into a term containing $2\leftrightarrow 2$ processes and a second term involving number-changing $2\leftrightarrow 4$ processes. While the number-changing processes are higher order in the coupling constant (λ), they are required in order for a system undergoing a uniform

[7] This is easily seen by using the definition of the sound speed,

$$c_s^2 = \frac{\frac{1}{3}\int\frac{d^3\mathbf{p}}{(2\pi)^3}p^2 n_\mathbf{p}(1\pm n_\mathbf{p})}{\int\frac{d^3\mathbf{p}}{(2\pi)^3}\tilde{E}_\mathbf{p}^2 n_\mathbf{p}(1\pm n_\mathbf{p})}. \tag{48}$$

[8] For our discussion, it will be sufficient to look at a pure $\lambda\phi^4$ theory.

expansion or contraction to equilibrate. If number-changing processes were not included, the above Boltzmann equation would have no solution. Formally, this is due to the presence of a (spurious) zero mode associated with particle-number conservation in the $2 \leftrightarrow 2$ processes. This zero mode is not orthogonal to the source term and subsequently renders the linearized Boltzmann equation noninvertible. We should also point out that there is a zero mode corresponding to energy conservation. This zero mode is not problematic since it is orthogonal to the source.

It is precisely the above behavior of a scalar field theory that allows one to obtain the approximate form of the off-equilibrium distribution function. In order to see how this works out, let us start by linearizing the above Boltzmann equation around its equilibrium solution

$$\delta f(\mathbf{p}) = -n_{\mathbf{p}}(1+n_{\mathbf{p}})\chi_\pi(p)\hat{p}^i\hat{p}^j\langle\partial_i u_j\rangle \\ -n_{\mathbf{p}}(1+n_{\mathbf{p}})\chi_\Pi(p)\partial_k u^k. \qquad (51)$$

This equation for δf follows from the Chapman-Enskog expansion Eq. (17). The equations in the shear and bulk channels can be separated. In the spin-0 (bulk) channel, we find

$$\frac{\beta}{E_{\mathbf{p}}}\left(\frac{p^2}{3} - c_s^2 E_{\mathbf{p}}\frac{\partial(\beta E_{\mathbf{p}})}{\partial\beta}\right) = -\mathcal{C}_{2\leftrightarrow 2}[\delta f,\mathbf{p}] - \mathcal{C}_{2\leftrightarrow 4}[\delta f,\mathbf{p}], \qquad (52)$$

where we have written $\mathcal{C}[\delta f, \mathbf{p}]$ to make it explicit that the collision term should be linearized around the equilibrium solution. The resulting operators (including the final-state symmetry factors) are

$$C_{2\leftrightarrow 2}[\delta f,\mathbf{p}] = \frac{1}{2!}\int_{\mathbf{k},\mathbf{p}',\mathbf{k}'}\Gamma_{\mathbf{pk}\to\mathbf{p}'\mathbf{k}'}\;n_{\mathbf{p}}n_{\mathbf{k}}(1+n_{\mathbf{p}'})(1+n_{\mathbf{k}'}) \\ \times[\chi_\Pi(p)+\chi_\Pi(k)-\chi_\Pi(p')-\chi_\Pi(k')], \quad (53)$$

$$C_{2\leftrightarrow 4}[\delta f,\mathbf{p}] \\ = \frac{1}{3!2!}\int_{\mathbf{k},\mathbf{p}',\mathbf{k}',\mathbf{q},\mathbf{q}'}\Gamma_{\mathbf{p}'\mathbf{k}\to\mathbf{pk}'\mathbf{qq}'}\;n_{\mathbf{p}}n_{\mathbf{k}'}n_{\mathbf{q}}n_{\mathbf{q}'}(1+n_{\mathbf{p}'})(1+n_{\mathbf{k}}) \\ \times[\chi_\Pi(p')+\chi_\Pi(k)-\chi_\Pi(p)-\chi_\Pi(k')-\chi_\Pi(q)-\chi_\Pi(q')] \\ -\frac{1}{4!1!}\int_{\mathbf{k},\mathbf{p}',\mathbf{k}',\mathbf{q},\mathbf{q}'}\Gamma_{\mathbf{pk}\to\mathbf{p}'\mathbf{k}'\mathbf{qq}'}\;n_{\mathbf{p}'}n_{\mathbf{k}'}n_{\mathbf{q}}n_{\mathbf{q}'}(1+n_{\mathbf{p}})(1+n_{\mathbf{k}}) \\ \times[\chi_\Pi(p)+\chi_\Pi(k)-\chi_\Pi(p')-\chi_\Pi(k')-\chi_\Pi(q)-\chi_\Pi(q')], \qquad (54)$$

where we have used the shorthand $\int_{\mathbf{p}} = \int\frac{d^3\mathbf{p}}{(2\pi)^3}$. The transition rates are given as

$$\Gamma_{\mathbf{pk}\to\mathbf{p}'\mathbf{k}'} = \frac{|\mathcal{M}_{2\to 2}|^2}{(2E_{\mathbf{p}})(2E_{\mathbf{k}})(2E_{\mathbf{p}'})(2E_{\mathbf{k}'})}(2\pi)^4\delta^4 \\ \times(P+K-P'-K'), \qquad (55)$$

$$\Gamma_{\mathbf{pk}\to\mathbf{p}'\mathbf{k}'\mathbf{qq}'} = \frac{|\mathcal{M}_{2\to 4}|^2}{(2E_{\mathbf{p}})(2E_{\mathbf{k}})(2E_{\mathbf{p}'})(2E_{\mathbf{k}'})(2E_{\mathbf{q}})(2E_{\mathbf{q}'})}(2\pi)^4\delta^4 \\ \times(P+K-P'-K'-Q-Q'). \qquad (56)$$

Formally, we can solve Eq. (52) by inverting the collision operator. Lu and Moore observed that the largest contribution will come from the near-zero mode [37], which has the form

$$\chi_\Pi(p) = \chi_0 - \chi_1 E_p, \qquad (57)$$

where χ_i are constants to be determined. By substituting the above form of $\chi_\Pi(p)$ into the spin-0 channel of the linearized Boltzmann equation (52), and integrating both sides over all phase space, we obtain

$$\chi_0 = \frac{\beta\mathcal{F}}{4\Gamma_{\text{inelastic}}}, \qquad (58)$$

where

$$\Gamma_{\text{inelastic}} = \frac{1}{48}\int_{\mathbf{pkp}'\mathbf{k}'\mathbf{qq}'}\Gamma_{\mathbf{pk}\to\mathbf{p}'\mathbf{k}'\mathbf{qq}'}\;n_{\mathbf{p}'}n_{\mathbf{k}'}n_{\mathbf{q}}n_{\mathbf{q}'} \\ \times(1+n_{\mathbf{p}})(1+n_{\mathbf{k}}), \qquad (59)$$

and we have defined the function

$$\mathcal{F} \equiv \int\frac{d^3\mathbf{p}}{(2\pi)^3E_{\mathbf{p}}}\left(\frac{p^2}{3} - c_s^2E_{\mathbf{p}}\frac{\partial(\beta E_{\mathbf{p}})}{\partial\beta}\right)n_{\mathbf{p}}(1+n_{\mathbf{p}}), \qquad (60)$$

which characterizes the deviation of the theory from conformality. The total inelastic cross section given in Eq. (59) can be computed by doing the phase-space integrals numerically. From a phenomenological perspective, this is not necessary. Instead, the total inelastic cross section can be related to the bulk viscosity coefficient by using Eq. (37). This identification leads to

$$\chi_0 = \frac{\zeta}{\mathcal{F}}. \qquad (61)$$

The constant χ_1 is undetermined by the Boltzmann equation. Instead, it is constrained by requiring that the deviation from equilibrium does not bring about a shift in the energy density,

$$\delta\epsilon = 0 = \int\frac{d^3\mathbf{p}}{(2\pi)^3E_{\mathbf{p}}}\tilde{E}_{\mathbf{p}}^2\delta f. \qquad (62)$$

We therefore find the following form for the off-equilibrium distribution function:

$$\chi_\Pi(p) = \frac{\zeta}{\mathcal{F}}(1-\mathcal{G}E_{\mathbf{p}}), \qquad (63)$$

where $\mathcal{F}$ has been defined in Eq. (60) and

$$\mathcal{G} \equiv \frac{\int\frac{d^3\mathbf{p}}{(2\pi)^3E_{\mathbf{p}}}\tilde{E}_{\mathbf{p}}^2n_{\mathbf{p}}(1+n_{\mathbf{p}})}{\int\frac{d^3\mathbf{p}}{(2\pi)^3}\tilde{E}_{\mathbf{p}}^2n_{\mathbf{p}}(1+n_{\mathbf{p}})}. \qquad (64)$$

For completeness, it is worth discussing the parametric behavior of the bulk viscosity at high temperature. The bulk viscosity coefficient is given by

$$\zeta = \frac{\beta\mathcal{F}^2}{4\Gamma_{\text{inelastic}}}. \qquad (65)$$

In the high-temperature limit, we can evaluate $\mathcal{F}$ semianalytically (see Appendix B2). In this regime, we can ignore the bare and thermal mass of the scalar quasiparticles (up to logarithms). The deviation from conformality contained in $\mathcal{F}$

is controlled by the running of the coupling. For a scalar field theory, we have

$$m^2_{\rm thermal} = \frac{\lambda T^2}{24} \longrightarrow \tilde{m}^2 = \frac{\beta(\lambda)T^2}{48}, \tag{66}$$

and using $\beta(\lambda) = \frac{3\lambda^2}{16\pi^2}$, we find that

$$\mathcal{F} = \frac{\lambda^2 T^4 \ln(\gamma\lambda)}{3(32\pi^2)^2} \quad \text{where} \quad \gamma \equiv \frac{1}{96} e^{15\zeta_+(3)/\pi^2}. \tag{67}$$

Naively, the total inelastic rate would go as $\lambda^4 T^4$. However, there is a soft enhancement which leads to $\Gamma \propto \lambda^3 T^4$ [35]. We therefore find that

$$\zeta \propto \frac{\lambda^3 T^3 \ln^2(\gamma\lambda)}{9(32\pi^2)^4}. \tag{68}$$

V. LEADING-LOG TREATMENT IN QCD

In this section, we will use the Boltzmann equation in the leading-log(T/m_D) approximation. In this approximation, the dynamics can be summarized by a Fokker-Plank equation which describes the momentum diffusion of the quasiparticles. The functional form of χ_Π can be found by solving a simple ordinary differential equation. We start by discussing the pure glue theory and then consider a multicomponent quark-gluon plasma (QGP).

A. Pure glue

In a leading-log approximation, $\log(T/m_D)$ is considered to be parametrically large. The resulting dynamics describes Coulomb scattering with a small momentum transfer of order $q \sim gT$, but with a rapid collision rate of $\sim g^2T$ (up to logarithms). At leading-log order, the linearized Boltzmann equation can be recast as a Fokker-Planck equation [38,39]. This equation allows us to determine $\chi(p)$ in a suitable limit (absence of "gain" terms) by solving a differential equation rather than an integral equation. The Fokker-Planck equation is

$$\begin{aligned}\frac{1}{2}p^i p^j \sigma_{ij} + \partial_i u^i \left(\frac{p^2}{3} - c_s^2 E_{\mathbf p}\frac{\partial(\beta E_{\mathbf p})}{\partial\beta}\right) \\ = \frac{T\mu_A}{n_{\mathbf p}(1+n_{\mathbf p})}\frac{\partial}{\partial \mathbf{p}^i}\left(n_{\mathbf p}(1+n_{\mathbf p})\frac{\partial}{\partial \mathbf{p}^i}\left[\frac{\delta f(\mathbf p)}{n_{\mathbf p}(1+n_{\mathbf p})}\right]\right) \\ + \frac{\text{gain terms}}{n_{\mathbf p}(1+n_{\mathbf p})},\end{aligned} \tag{69}$$

where μ_A is the drag coefficient in the leading-log approximation

$$\frac{d\mathbf p}{dt} = \mu_A \hat{\mathbf p}, \qquad \mu_A = \frac{g^2 C_A m_D^2}{8\pi}\log\left(\frac{T}{m_D}\right). \tag{70}$$

The Debye mass is given by $m_D^2 = \frac{1}{3}(C_A + \frac{N_f}{2})g^2T^2$ with $C_A = N_c$. Equation (69) without the gain terms is a Fokker-Planck equation for a hard particle undergoing drag and diffusion in a thermal bath. In order to conserve energy and momentum, the gain terms must be included. The gain terms can be written as [38]

$$\begin{aligned}\text{gain terms} \equiv \frac{6}{T^3}\left[\frac{1}{p^2}\frac{\partial}{\partial p}p^2 n_{\mathbf p}(1+n_{\mathbf p})\right]\frac{dE}{dt} \\ + \frac{6}{T^3}\left[\frac{\partial}{\partial \mathbf p}n_{\mathbf p}(1+n_{\mathbf p})\right]\cdot\frac{d\mathbf P}{dt},\end{aligned} \tag{71}$$

where dE/dt and $d\mathbf P/dt$ are the energy and momentum transfer to the hard particle from the thermal bath per unit time;

$$\frac{dE}{dt} = \int \frac{d^3\mathbf p}{(2\pi)^3}\hat{\mathbf p}\cdot\mathbf j_p, \qquad \frac{d\mathbf P}{dt} = \int\frac{d^3\mathbf p}{(2\pi)^3}\mathbf j_p, \tag{72}$$

where

$$\mathbf j_p = -T\mu_A n_{\mathbf p}(1+n_{\mathbf p})\frac{\partial}{\partial \mathbf p}\left[\frac{\delta f}{n_{\mathbf p}(1+n_{\mathbf p})}\right]. \tag{73}$$

We express the off-equilibrium distribution function in terms of χ_π and χ_Π as in Eq. (51). By substituting this expression into the Fokker-Planck equation, we find that the shear and bulk contributions decouple. In the shear channel, the gain terms vanish and we are left with the following ordinary differential equation for $\chi_\pi(p)$:

$$\frac{p}{T} = \mu_A T\left[-\chi_\pi'' + \left(\frac{1+2n_{\mathbf p}}{T} - \frac{2}{p}\right)\chi_\pi' + \frac{6}{p^2}\chi_\pi\right]. \tag{74}$$

At high momentum, $(1+2n_{\mathbf p}) \to 1$ and we find [29]

$$\chi_\pi(p) = \frac{1}{2T\mu_A}p^2. \tag{75}$$

The above differential equation can also be solved numerically. For this purpose, two boundary conditions must be specified. The first boundary condition is that $\chi_\pi(p=0)=0$, which implies that in QCD soft gluons equilibrate rapidly. The second boundary condition follows from the structure of the solution at large momentum. In general, the differential equation has two independent solutions, one being a polynomial in p and the other growing exponentially in p. We choose the second boundary condition so that the exponentially growing solution is suppressed. In practice, this can be done using a shooting method on $\chi'(p=0)$ such that $\chi'''(p=p_{\max})=0$, which removes the exponential solution. The result of this procedure is shown in Fig. 3. The shear viscosity can be found using the relation

$$\eta = \sum_a \frac{\nu_a}{30\pi^2}\int\frac{p^4}{E_{\mathbf p}}n_{\mathbf p}(1\pm n_{\mathbf p})\chi_\pi(p), \tag{76}$$

and we find $\eta/(g^4T^3\ln) = 27.1$ in agreement with [39].

In the case of bulk ($l=0$) channel, while $d\mathbf P/dt$ is zero the gain term dE/dt is nonvanishing. In order to understand the role of this term, we first analyze the Fokker-Planck without the gain term

$$\begin{aligned}\left(\frac{1}{3}-c_s^2\right)\frac{p}{T} - c_s^2\tilde{m}_A^2\frac{1}{pT} \\ = \mu_A T\left[-\chi_\Pi'' + \left(\frac{1+2n_{\mathbf p}}{T} - \frac{2}{p}\right)\chi_\Pi'\right].\end{aligned} \tag{77}$$

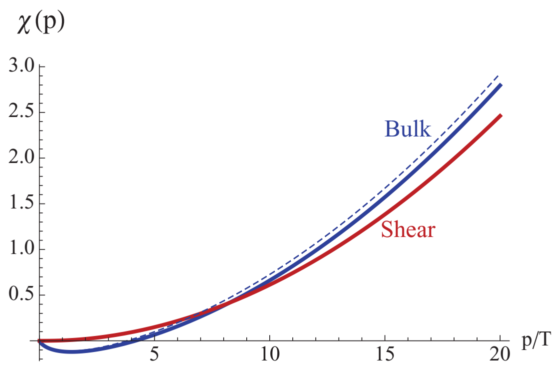

FIG. 3. (Color online) Nonequilibrium distribution functions χ_π (red curve labeled shear) and χ_Π (blue curves labeled bulk) of gluons in leading log approximation. The functions χ_π and χ_Π are defined in Eq. (51). We have rescaled χ_π by one power of the conformal breaking parameter $(1/3 - c_s^2)$ in order to check the expected scaling behavior $\chi_\Pi \sim (1/3 - c_s^2)\chi_\pi$. The dotted line shows the bulk viscous correction χ_Π before it was made orthogonal to the energy density. The curves in this plot were obtained for $m_D/T = 1$, corresponding to a very weak coupling $\alpha_s = 1/(4\pi)$.

This differential equation has one exact zero mode, $\chi_\Pi \propto$ const, related to particle-number conservation in $2 \leftrightarrow 2$ scattering. This zero mode is removed if $2 \leftrightarrow 3$ splitting and joining processes are included. We can take this into account by imposing the boundary condition $\chi_\Pi(p = 0) = 0$. The second boundary condition is chosen in order to suppress the exponentially growing solution as discussed in the shear case.

The solution obtained in this way is not physically acceptable because it does not respect energy conservation. The fact that the collision term conserves energy implies that the most general solution of the linearized Boltzmann equation must be of the form $\chi_\Pi(p) = \chi_\Pi^0(p) + \chi^1 p$, where χ^1 is a constant and we have used the fact that the leading-log collision integral is computed using $E_p \simeq p$. It is easy to see that this is a property of the Fokker-Planck equation in the bulk channel with the gain term included, but not without it. We find that restoring the zero mode $\chi_\Pi \propto p$ is the dominant effect of the gain term, and that $\chi_\Pi^0(p)$ is very well approximated by the solution of the ordinary differential equation (77).

The freedom in adding the zero mode has no effect on the calculation of the bulk viscous pressure via Eq. (37) because any shift in the pressure due to a shift in the energy density is projected out. However, in this work, we are also interested in the correction to the single-particle spectra, and in that context the linear term in χ_Π matters. We therefore fix χ^1 by the requirement that δf does not contribute to the energy density as required by the Landau-matching conditions

$$0 = \int \frac{d^3\mathbf{p}}{(2\pi)^3 E_\mathbf{p}} \tilde{E}_\mathbf{p}^2 n_\mathbf{p}(1 + n_\mathbf{p})[\chi_\Pi(p) - \chi^1 p]. \quad (78)$$

In this case, there is no need to remove the shift in pressure due to the shift in energy density when computing the bulk viscosity

$$\zeta = \int \frac{d^3\mathbf{p}}{(2\pi)^3 E_\mathbf{p}} \frac{p^2}{3} n_\mathbf{p}(1 + n_\mathbf{p})[\chi_\Pi(p) - \chi^1 p]. \quad (79)$$

The numerical solution of Eq. (77) is shown in Fig. 3. We observe that χ_B changes sign at $p \sim 4T$, and that for large values of the momentum $p \gtrsim 7T$, the nonequilibrium distribution function in the bulk channels scales as the distribution function in the shear channel multiplied by one power of the conformal symmetry-breaking parameter

$$\chi_\Pi \sim \left(\tfrac{1}{3} - c_s^2\right)\chi_\pi. \quad (80)$$

Integrating the solution gives $\zeta/(T^3\alpha_s^2)\ln = 0.44$, in agreement with the result in [11]. The bulk viscosity scales as the second power of the conformal symmetry parameter

$$\zeta \sim 47.9\left(\tfrac{1}{3} - c_s^2\right)^2 \eta. \quad (81)$$

This result has the same structure as the relation obtained in the relaxation time approximation [Eq. (41)], but with a larger numerical coefficient.

B. Quark-gluon plasma

The previous analysis can be easily extended to a multicomponent system. For a quark-gluon plasma, the extension of Eq. (77) is [38,39]

$$q_A(p) = \mathcal{C}_{\text{Loss}}(\chi^g) - \frac{2\gamma}{p}\frac{N_f d_F}{d_A}\frac{n_\mathbf{p}^F}{n_\mathbf{p}^B}(\chi^q + \chi^{\bar{q}} - 2\chi^g), \quad (82)$$

$$2q_F(p) = \mathcal{C}_{\text{Loss}}(\chi^q) + \mathcal{C}_{\text{Loss}}(\chi^{\bar{q}}) + \frac{2\gamma}{p}(\chi^q + \chi^{\bar{q}} - 2\chi^g)\left[\frac{1 + n_\mathbf{p}^B}{1 - n_\mathbf{p}^F}\right], \quad (83)$$

$$0 = \mathcal{C}_{\text{Loss}}(\chi^q) - \mathcal{C}_{\text{Loss}}(\chi^{\bar{q}}) + \frac{2\gamma}{p}(\chi^q - \chi^{\bar{q}})\left[\frac{1 + n_\mathbf{p}^B}{1 - n_\mathbf{p}^F}\right], \quad (84)$$

where $\chi^{g,q} = \chi_\Pi^{g,q}(p)$ is the off-equilibrium distribution function for gluons and quarks, and $q_{I=A,F}$ is the corresponding source term (A adjoint gluons, F fundamental quarks). The source and loss terms are different in the shear ($l = 2$) and bulk ($l = 0$) channels. In the bulk channel,

$$q_I(p) \equiv \left(\frac{1}{3} - c_s^2\right)\frac{p}{T} - c_s^2 \tilde{m}_I^2 \frac{1}{pT}, \quad (85)$$

$$\mathcal{C}_{\text{Loss}}(\chi) \equiv \mu_I T\left[-\chi'' + \left(\frac{1 \pm 2n_\mathbf{p}}{T} - \frac{2}{p}\right)\chi'\right]. \quad (86)$$

For comparison, we also show the corresponding source and loss term in the shear channel,

$$q_I(p) \equiv \frac{p}{T}, \quad (87)$$

$$\mathcal{C}_{\text{Loss}}(\chi) \equiv \mu_I T\left[-\chi'' + \left(\frac{1 \pm 2n_\mathbf{p}}{T} - \frac{2}{p}\right)\chi' + \frac{6}{p^2}\chi\right]. \quad (88)$$

The coupled second-order differential equations for $\chi^{g,q}$ can be solved in the same manner as the pure glue case. The

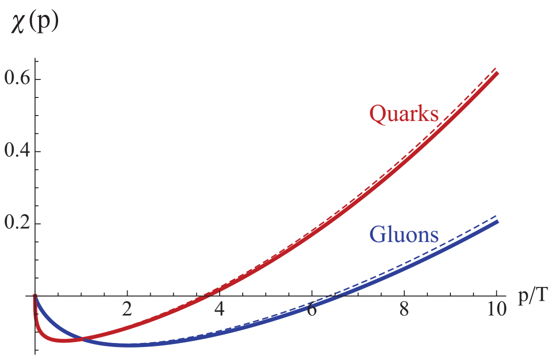

FIG. 4. (Color online) Deviation of quarks and gluons from equilibrium due to a bulk stress in leading-log approximation. The dashed curves show the results before the solutions were made orthogonal to the energy density.

result is shown in Fig. 4. We observe that there are important differences between quarks and gluons, and that there is a shift in the gluon distribution due to the presence of quarks. Integrating the distribution functions gives a bulk viscosity $\zeta/(T^3\alpha_s^2)\ln = 0.66$ for $N_f = 3$.

We are now in a position to compute viscous corrections to the elliptic flow of quarks and gluons. Our calculations are based on the (2 + 1)-dimensional second-order hydrodynamics code described in [2]. See Appendix A for details of the hydrodynamic model. We choose an initial energy density appropriate for Au + Au collisions at 200 A GeV. The results shown in Fig. 5 correspond to an impact parameter $b = 6.8$ fm. The differential elliptic flow parameter $v_2(p_T)$ for quarks and gluons is computed using the strategy outlined in the Introduction. We have used $m_D = 2.9T$, which corresponds to $c_s^2 = 0.2$. For these parameters, leading-log QCD predicts $\eta/s = 0.16$ and $\zeta/s = 0.08$. These values of the transport coefficients lead to rather large corrections of the spectra. The results shown in Fig. 5 were obtained for a smaller value of the bulk viscosity $\zeta/s = 0.04$.

In both the left and the right panels of Fig. 5, the elliptic flow parameter $v_2(p_T)$ in ideal hydrodynamics is shown as the solid red line, and the elliptic flow of quarks and gluons in a simulation with shear viscosity only is shown as the solid green and blue curves. The dashed curves in the left panel show the result if bulk viscosity is included in the hydrodynamic evolution, but not in the distribution functions (shear viscosity is included in δf). We note that this procedure violates energy-momentum conservation across the freeze-out hypersurface, but it gives an indication of the role that bulk viscosity plays in the hydrodynamic evolution. The inclusion of bulk viscosity reduces both the radial flow and the momentum anisotropy. These two effects lead to a small reduction of $v_2(p_T)$ for $p_T \lesssim 2$ GeV.

The right panel in Fig. 5 shows the full result including the effect of bulk viscosity on the distribution function. Comparing with the left panel, we clearly observe the importance of viscous correction to δf. From Eq. (51) and Fig. 4, we can see that the shift in the distribution functions due to bulk viscosity is positive at small p_T. From Fig. 4, the sign change in χ_Π occurs around $p/T \sim 5$. At a decoupling temperature of 150 MeV, this corresponds to $p_T \lesssim 750$ MeV. Taking into account the boost due to radial expansion, the critical p_T is further reduced to $p_T \lesssim 400$ MeV, which is barely visible on the plot. At higher momentum, the bulk viscosity tends to soften the p_T spectra. As the spectra enter into the denominator in Eq. (10), this leads to an increase in $v_2(p_T)$.

Overall, the effect of bulk viscosity on $v_2(p_T)$ in the regime $p_T \lesssim 2$ GeV is modest, considering that ζ is only a factor of four smaller than η. This result is consistent with the scaling relations (80) and (81). At very weak coupling, ζ is suppressed by two powers of the small parameter $(1/3 - c_s^2)$, whereas δf is only suppressed by one power. At strong coupling, however, the large numerical coefficient in Eq. (81) enhances ζ/η relative to χ_Π/χ_π.

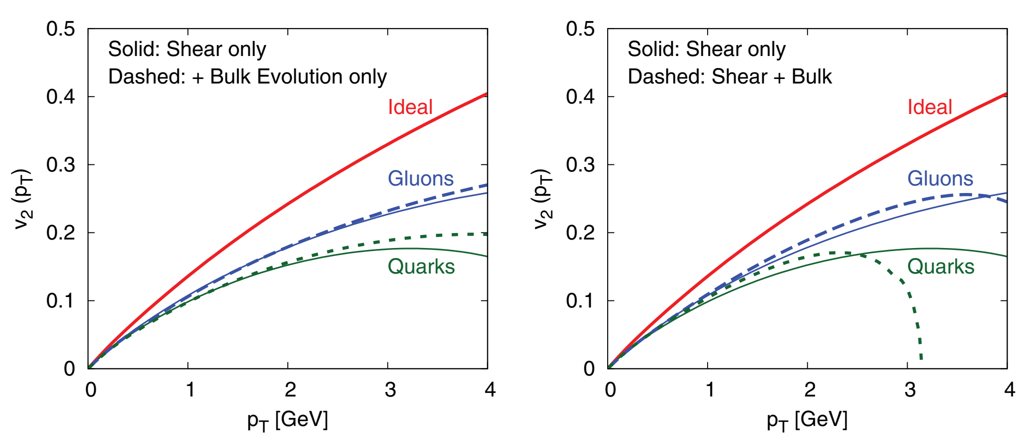

FIG. 5. (Color online) Differential elliptic flow of quarks and gluons. The solid curves labeled "quarks" and "gluons" represent the quark and gluon elliptic flow using the leading-log form of the shear viscous correction to the distribution function. In both figures, the shear viscosity to entropy ratio is $\eta/s = 0.16$. The corresponding dashed curves are the results for a viscous hydrodynamic evolution having $\eta/s = 0.16$ and $\zeta/s = 0.04$. The dashed curves in the left plot neglect the bulk viscous correction to the distribution function at freeze-out. The left plot should be taken as strictly pedagogical since energy-momentum conservation is violated. The right plot shows the complete leading-log result. Additional details of the hydrodynamic parameters can be found in Appendix A.

C. Leading-order behavior at large momentum

In perturbative QCD, the leading-order result for the bulk viscosity is governed by small-angle $2 \leftrightarrow 2$ scattering, and inelastic $2 \leftrightarrow 3$ processes are suppressed by a logarithm of the coupling constant. At large momenta, $p > T/\ln(1/g)$, the logarithmic suppression is compensated by the growth of the $2 \leftrightarrow 3$ reaction with energy. In this regime, the correction to the distribution function is determined by the physics of energy loss. Arnold *et al.* showed that at leading order in the coupling, these effects can be included in terms of an effective $1 \leftrightarrow 2$ collision term [40]

$$\begin{aligned}\frac{p\nu_a \mathcal{C}_a^{1\leftrightarrow 2}}{(2\pi)^3} =& \sum_{bc}\int \frac{dx}{x^{5/2}}\,\gamma^c_{ab}[p;xp,(1-x)p] \\ &\times n^a_{\mathbf{p}} n^b_{(1-x)\mathbf{p}/x}\big(1\pm n^c_{\mathbf{p}/x}\big)\big[\chi^a_p+\chi^b_{(1-x)p/x}-\chi^c_{p/x}\big] \\ &+\frac{1}{2}\sum_{bc}\int dx\,\gamma^a_{bc}[p;xp,(1-x)p]n^a_{\mathbf{p}}\big(1\pm n^b_{x\mathbf{p}}\big) \\ &\times\big(1\pm n^c_{(1-x)\mathbf{p}}\big)\big[\chi^a_p-\chi^b_{xp}-\chi^c_{(1-x)p}\big], \end{aligned} \tag{89}$$

where $a,b,c = g,q$ for quarks/gluons and $\chi_p \equiv \chi_\sqcap(p)$. The splitting functions γ^a_{bc} are given by

$$\gamma^g_{gg} = \sqrt{2\hat{q}}\,\frac{\alpha_s C_A d_A}{(2\pi)^4}\sqrt{1+x^2+(1-x)^2}\,\frac{1+x^4+(1-x)^4}{[x(1-x)]^{3/2}}, \tag{90}$$

$$\gamma^g_{qq} = \sqrt{2\hat{q}}\,\frac{\alpha_s C_F d_F}{(2\pi)^4}\sqrt{\kappa+x^2+(1-x)^2}\,\frac{x^2+(1-x)^2}{[x(1-x)]^{1/2}}, \tag{91}$$

$$\gamma^q_{gq} = \sqrt{2\hat{q}}\,\frac{\alpha_s C_F d_F}{(2\pi)^4}\sqrt{1+\kappa x^2+(1-x)^2}\,\frac{1+(1-x)^2}{[x^3(1-x)]^{1/2}}, \tag{92}$$

where $\kappa \equiv (2C_F - C_A)/C_A$ and

$$\hat{q} = C_A g^2 T m_D^2 \int \frac{d^2q_\perp}{(2\pi)^2}\frac{1}{q_\perp^2+m_D^2} = C_A\alpha_s T m_D^2 \ln\left(\frac{\langle k_T^2\rangle}{m_D^2}\right) \tag{93}$$

is the transverse diffusion constant that controls energy loss in a quark-gluon plasma. We can study the effect of the $1 \leftrightarrow 2$ splitting term on the solution of the Boltzmann equation in the bulk channel at large p_T. We find that the asymptotic form of $\chi_\sqcap$ is suppressed relative to the asymptotic solution for χ_π by the first power of the conformal symmetry-breaking parameter

$$\chi^a_\sqcap(p) = \left(\tfrac{1}{3}-c_s^2\right)\chi^a_\pi(p) \quad \text{for} \quad p \gg T\ln^{-1}(1/g). \tag{94}$$

The asymptotic form of the gluon distribution in the shear channel is given by

$$\chi^g_\pi(p) \approx \frac{0.7}{\alpha_s T\sqrt{\hat{q}}}\,p^{3/2}, \tag{95}$$

where we have used $N_f = 0$. The corresponding result for the quark distribution, as well as the dependence on the number of flavors, is given in [29].

VI. HADRONIC GAS

In the previous section, we saw that there are significant differences between the viscous corrections to the differential elliptic flow of quarks and gluons. Of course, the spectra of quarks and gluons are not directly observable. In this section, we study the question as to whether similar differences are expected in the spectra and $v_2(p_T)$ of different hadronic species.

A. Low-temperature pion gas

The bulk viscosity of a pion gas was studied by a number of authors [37,41–43]. Lu and Moore argued that the system is similar to the scalar field theory studied in Sec. IV, and that the bulk viscosity is controlled by number-changing processes [37]. We will therefore follow the discussion leading up to Eq. (57) and assume that the deviation from equilibrium is governed by the near-zero mode

$$\chi(p) = \chi_0 - \chi_1 E_p. \tag{96}$$

The coefficient χ_1 is determined by Landau matching, and the coefficient χ_0 is controlled by the inelastic cross section

$$\chi_0 = \frac{\beta\mathcal{F}}{4\Gamma_{\text{inelastic}}}, \tag{97}$$

where $\mathcal{F}$ as written in Eq. (60) is a measure of the deviation from conformal behavior. In the case of a pion gas, we will ignore mean-field effects ($\tilde{m}_\pi = m_\pi$), and take the deviation from conformality to be driven by the bare mass of the pion. In this case, $\mathcal{F}$ takes the form

$$\mathcal{F} = \int \frac{d^3\mathbf{p}}{(2\pi)^3 E_{\mathbf{p}_\pi}}\left(\frac{p^2}{3} - c_s^2 E^2_{\mathbf{p}_\pi}\right) n_{\mathbf{p}}(1+n_{\mathbf{p}}). \tag{98}$$

The total inelastic rate is dominated by the lowest-order number-changing process, which is kinematically allowed: $\pi\pi \leftrightarrow \pi\pi\pi\pi$. The inelastic cross section also controls the chemical equilibration rate of pions. The rate at which a pion chemical potential will return to equilibrium is given by [44]

$$\frac{1}{\tau_\pi^{\text{chem}}} = \frac{\sum_i \left(\delta n_i^\pi\right)^2\ \Gamma_i}{n_\pi}, \tag{99}$$

where the sum is over all reactions which increase the pion number by δn_i^π. We can therefore make the following identification between the bulk viscosity and chemical relaxation time:

$$\zeta = \frac{\mathcal{F}^2}{n_\pi}\tau_\pi^{\text{chem}}. \tag{100}$$

If we use classical statistics, which is valid for $m_\pi \gg T$, the phase-space integrals appearing in $\mathcal{F}$ can be evaluated analytically. Normalizing the bulk viscosity by the entropy density, we arrive at the following relationship between the bulk viscosity of a low-temperature pion gas and the chemical equilibration rate:

$$\frac{\zeta}{s} = \frac{m_\pi}{K_2\,K_3}\left(\frac{K_2^2 - K_1\,K_3}{3K_3+\beta m_\pi K_2}\right)^2 \tau_\pi^{\text{chem}}, \tag{101}$$

where $K_{i=1,2,3}$ is the modified Bessel function of order $i = 1, 2, 3$ evaluated at (βm_π). The chemical reaction time arising from inelastic pion reactions can be computed in chiral perturbation theory. For example, the work of [45] (see also [46]) found $\tau_\pi^{\text{chem.}} = 450$ fm/c at $T = 140$ MeV and $\tau_\pi^{\text{chem.}} = 120$ fm/c at $T = 160$ MeV for a pion mass $m_\pi = 138$ MeV. Based on these calculations, we find $\zeta/s \approx 0.14$ at $T = 140$ MeV and $\zeta/s \approx 0.03$ at $T = 160$ MeV.

B. Hadronic resonance gas

The estimate of ζ for a pure pion gas is likely to be relevant only in a relatively small temperature regime. In the regime between the freeze-out and the critical temperature, many resonances are important. We will assume that the bulk viscosity of a hadronic resonance gas is also dominated by number-changing processes. If this is the case, we may approximate the deviation from equilibrium due to bulk viscosity for each hadronic species by the near-zero mode

$$\delta f^a(\mathbf{p}) = -n_{\mathbf{p}}^a\left(1 \pm n_{\mathbf{p}}^a\right)\partial_k u^k \left(\chi_0^a - \chi_1 E_{\mathbf{p}_a}\right), \tag{102}$$

where $E_{\mathbf{p}_a} = \sqrt{p^2 + m_a^2}$. The coefficient χ_1 (which is the same for all species) is determined by the Landau-matching condition

$$\delta\epsilon = 0 = \sum_a \nu_a \int \frac{d^3\mathbf{p}}{(2\pi)^3} E_{\mathbf{p}_a} \delta f^a(\mathbf{p}), \tag{103}$$

where $a = \pi, K, \ldots$ is a sum of all hadronic species in a resonance gas having degeneracy ν_a. Using the generalization of Eq. (37) to a system of multiple species, we find

$$\zeta = \sum_a \nu_a \chi_0^a \mathcal{F}^a, \tag{104}$$

where

$$\mathcal{F}^a = \int \frac{d^3\mathbf{p}}{(2\pi)^3 E_{\mathbf{p}_a}} \left(\frac{p^2}{3} - c_s^2 E_{\mathbf{p}_a}^2\right) n_{\mathbf{p}}^a\left(1 \pm n_{\mathbf{p}}^a\right). \tag{105}$$

As in the case of a dilute pion gas, we neglect mean-field effects and assume that the deviation from conformality is related to the bare masses of the resonances. The off-equilibrium distribution in a multicomponent system is determined by one parameter χ_1, which is common to all species, and N_{species} parameters χ_0^a that are different for each species. The parameter χ_1 is determined by the Landau-matching condition, and one linear combination of the χ_0^a can be related to the bulk viscosity. Explicit information on inelastic hadronic cross sections is needed to determine the remaining $(N_{\text{species}} - 1)$ coefficients.

In this work, we will not attempt to compute these inelastic rates. Instead, we will rely on a model that is motivated by prior calculations of chemical equilibration rates in a hadronic resonance gas [44–48]. By using a phenomenological model for the inelastic cross section, Pratt and Haglin showed that the chemical equilibration time near thermal freeze-out is 5–10 times larger for kaons than it is for pions [44]. A similar estimate was also obtained in a Boltzmann-Uehling-Uhlenbeck (BUU) transport model [47]. We therefore expect the bulk viscous correction of kaons to be that much larger than pions (i.e., $\chi_0^K/\chi_0^\pi \sim 5$–10.). A larger set of resonances (but excluding strangeness) was studied by Goity [45]. In this paper, the deviation from chemical equilibrium (at fixed temperature) is parametrized in terms of effective chemical potentials for nonconserved charges such as the total number of pions, rho mesons, nucleons plus antinucleons, etc. Goity finds that the largest relaxation time corresponds to a chemical potential for meson (baryon) resonances approximately twice (2.5 times) larger than that of pions near the transition temperature.

In the following, we will use the ansatz in Eq. (102) and choose χ_0^a for each meson and baryon species to be a constant multiple C_m and C_b of χ_0^π:

$$\chi_0^a = \begin{cases} \chi_0^\pi & \text{pions,} \\ C_m \times \chi_0^\pi & \text{mesons,} \\ C_b \times \chi_0^\pi & \text{baryons.} \end{cases} \tag{106}$$

Due to the strong $\rho \to 2\pi$ reaction rate, we expect the ρ and π mesons to be in relative chemical equilibrium. This suggests that $\mu_\rho = 2\mu_\pi$ and therefore $C_m \approx 2$. Additionally, the average pion multiplicity in the strong $p\bar{p} \to n\pi$ reaction is $n \sim 5$ [49], so that $2\mu_N \approx 5\mu_\pi$ and therefore $C_b \approx 2.5$. These numbers are in good agreement with results obtained by Goity [45]. The remaining coefficient χ_0^π is related to the bulk viscosity via Eq. (104):

$$\zeta = \chi_0^\pi \sum_a \nu_a C_a \mathcal{F}^a \quad \text{where} \quad C_a = \begin{cases} 1 & \text{pions,} \\ C_m & \text{mesons,} \\ C_b & \text{baryons.} \end{cases} \tag{107}$$

We emphasize that in a complete calculation that includes inelastic rates such as $N\bar{N} \to 5\pi$, the value of ζ is completely determined by microscopic dynamics. Without microscopic information about inelastic rates, we can place bounds on χ_0^π from the observed spectra, and then extract bounds on ζ from Eq. (107).

Details of the hydrodynamic simulation are described in Appendix A. We use the same initial conditions and impact parameter as in the case of the pure QGP simulation. The equation of state is a parametrization of a lattice QCD equation of state [8]. In the kinetic model defined in Eq. (102), we include meson/baryon resonances up to a mass of 1.6 GeV (mesons) and 1.8 GeV (baryons). We have checked that the corresponding equation of state matches the lattice equation of state at freeze-out. Our resonance gas model implies $\chi_\pi^0 \simeq -100\zeta/(sT)$. We have chosen $(\zeta/s)_{\text{frzout}} = 0.005$, which corresponds to $\chi_p^0 \simeq -0.5/T$. Using the average expansion rate $(\partial_k u^k)$ at freeze-out, the value of χ_0^π can be translated into an effective pion chemical at freeze-out [see Eq. (109)]. We find $\mu_\pi \simeq 25$ MeV. This value is roughly consistent with the pion chemical potential $\mu_\pi \simeq 10$ MeV used in the thermal fireball model developed by Rapp [50].

We note that we use the same speed of sound, and therefore the same deviation from conformality, in our calculations in the quark-gluon plasma phase and the hadron resonance gas. The difference between the values of ζ/s in the two phases is connected with the different relations between χ_Π and ζ for the two

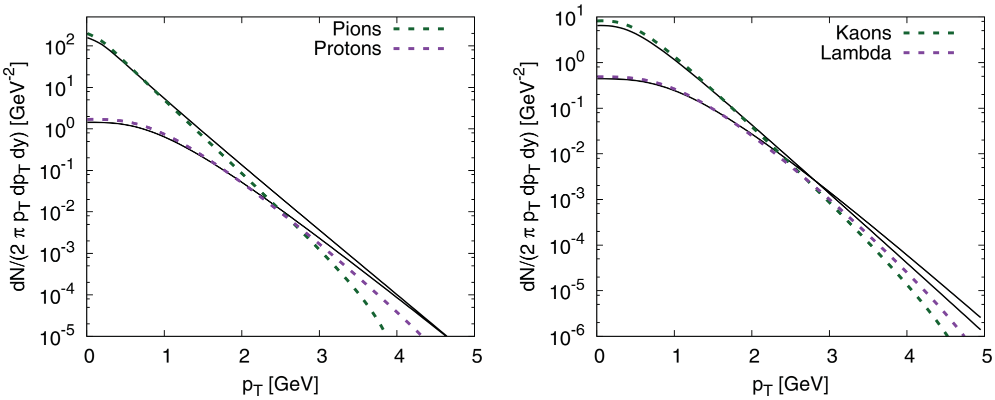

FIG. 6. (Color online) Transverse momentum spectra of pions, protons (left panel), as well as kaons and lambda baryons (right panel). The solid lines correspond to shear viscosity only, and the dashed lines show the result for shear and bulk viscosity with $\eta/s = 0.16$ and $\zeta/s = 0.005$.

systems. These relations reflect different physical mechanisms for producing bulk viscosity. In the quark-gluon plasma, bulk viscosity is controlled by momentum rearrangement, and shear and bulk viscosity are intimately related [see Eq. (81)]. In the hadron resonance gas model, bulk viscosity is dominated by particle-number changing processes, and there is no direct relation between shear and bulk viscosity. The fairly small value of ζ/s in the hadron resonance gas is further related to cancellations between low- and high-mass resonances in Eq. (105).

In Fig. 6, we show the p_T spectra of pions, protons, kaons, and lambdas. The shear viscosity was chosen to be $\eta/s = 0.16$ as in Fig. 5. Corrections to the hadronic spectra due to the shear viscosity were computed as described in [29]. We observe that, as in the case of quarks and gluons, bulk viscosity increases the spectra at small p_T, and suppresses the spectra at large p_T. The high-p_T suppression is more prominent in the case of pions because the spectra are determined by the competition between the constant term χ_0^a and the linear term $-\chi_1 E_{\mathbf{p}_a}$ term, where the constant contribution is bigger in the case of baryons, $\chi_0^B > \chi_0^\pi$.

While not obvious from Fig. 6, we should point out that the total particle number depends on the bulk viscous pressure [see Eq. (109)] and this shift in number density at freeze-out is species dependent. Particle ratios will therefore have a sensitivity to the bulk viscosity. Of course, any conserved quantity (such as baryon number) remains conserved. Since the off-equilibrium correction is the same for particles and antiparticles, the net baryon ($B - \overline{B}$) number remains unchanged. On the other hand, the total baryon number ($B + \overline{B}$) will deviate from its equilibrium value by an amount proportional to the bulk viscous pressure.

The effect of bulk viscosity on the elliptic flow parameter $v_2(p_T)$ is shown in Fig. 7. For comparison, we also show the elliptic flow from ideal hydrodynamics, and separately for a shear viscosity of ($\eta/s = 0.16$). We find that bulk viscosity tends to increase elliptic flow for $p_T \gtrsim 1$ GeV. The reason is the same as in Fig. 5: bulk viscosity suppresses the single-particle spectra at large p_T, and the spectra enter into the denominator of the definition of $v_2(p_T)$ [see Eq. (10)]. The effect becomes very large for $p_T \gtrsim 2.5$ GeV. A similar behavior was seen in [17]. Clearly, the large-p_T behavior is unphysical and stems from the fact that the particle distribution function becomes negative at some p_T. In order to circumvent this, we can attempt to do a resummation of the viscous correction. We can expand $f^a(\mathbf{p})$ to first order in δT and chemical potential μ,

$$\delta f^a(\mathbf{p}) = n^a_{\mathbf{p}}\big(1 \pm n^a_{\mathbf{p}}\big)\left(\frac{\mu^a}{T} + \frac{E_{\mathbf{p}_a}\delta T}{T^2}\right). \tag{108}$$

Comparing this with the form of the off-equilibrium distribution given in Eq. (102), we make the identification

$$\mu^a = -(\partial_k u^k) T \chi_0^a, \tag{109}$$

$$\delta T = +(\partial_k u^k) T^2 \chi_1. \tag{110}$$

The physics behind this is straightforward. As a system undergoes an expansion (in heavy-ion collisions the expansion rate is $\partial_k u^k \sim \frac{1}{\tau}$), the density of the system drops. However, due to the inefficiency of number-changing processes, there is an excess of particles with respect to what would be expected given the energy density of the system. This excess of particles can be parametrized by a positive shift in the chemical potential. We can resum the viscous correction by using the ideal distribution function with a shifted temperature and chemical potential[9]

$$f^a(\mathbf{p}) \approx \frac{1}{e^{\frac{E_{\mathbf{p}_a}}{T+\delta T} - \beta\mu^a} \pm 1}. \tag{111}$$

The above nonequilibrium distribution function is manifestly positive definite. The resulting v_2 spectrum is shown in the left panel of Fig. 7. At low p_T, the spectrum matches the linearized form, but it has the advantage that it is well behaved at high p_T.

Resumming the effects of bulk viscosity on the spectra is not as important if shear viscosity is also included. Shear viscosity tends to harden the p_T spectra, and therefore prevents the distribution function from becoming negative (provided η/s is sufficiently large). In the right panel of Fig. 7, we show the

[9]In our calculations, we have put the factor $e^{\mu^a/T}$ in the numerator in order to avoid possible problems with Bose condensation in certain regions of phase space.

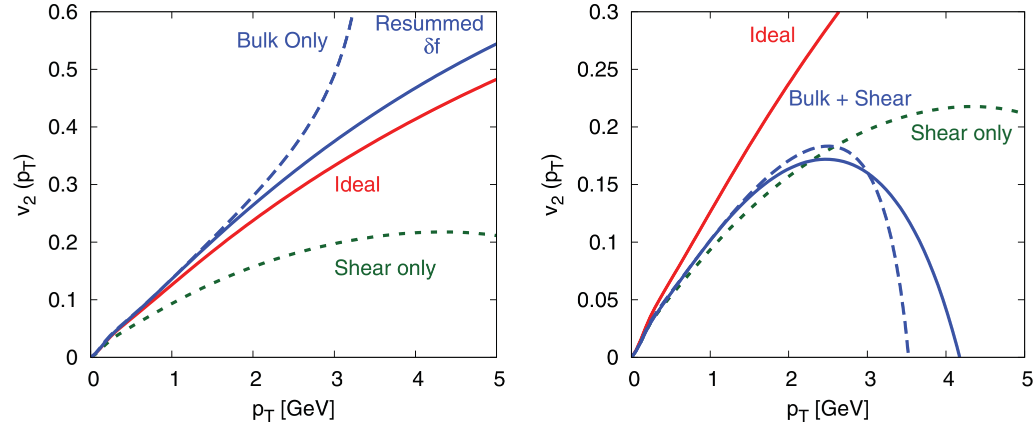

FIG. 7. (Color online) The left panel shows the elliptic flow of pions for a bulk viscosity at freeze-out of $(\zeta/s)_{\rm frzout} \approx 0.005$. The dashed curve shows the result using the linear form of the viscous correction given in Eq. (102), and the solid curve shows the result using the resummed form given in Eq. (111). The right panel shows the elliptic flow of pions from viscous hydrodynamics when both shear and bulk viscosity are included. The two curves labeled "bulk + shear" are labeled as in the left panel: the dashed line is the linear form of the distribution function, and the solid line shows the resummed result.

elliptic flow of pions when both shear and bulk viscosity are taken into account. In this case, we see much better agreement between the linear and resummed result even at large p_T. We observe that the effect of bulk viscosity on the pion $v_2(p_T)$ is comparable to the analogous correction to the quark $v_2(p_T)$, despite the smaller bulk viscosity used in our simulation of the hadronic phase. This is related to the larger numerical coefficient that appears in the relation between ζ and $(\frac{1}{3} - c_s^2)\chi(p)$ in the quark-gluon plasma compared to the hadron resonance gas.

In Fig. 8, we compare viscous corrections to the differential elliptic flow parameter $v_2(p_T)$ for different hadronic species. Reference [29] observed that a simple model for elastic meson and baryon cross section reproduces the empirically observed quark number scaling of $v_2(p_T)$. Figure 8 shows that bulk viscosity leads to significant modifications of the $v_2(p_T)$ of individual species, but the scaling relations between different species are approximately preserved.

At a fixed deviation from conformality, the off-equilibrium correction to the spectrum increases linearly with the bulk viscosity coefficient ζ. This means that the value of ζ can not be increased by very much without resulting in spectra and flow parameters that are in clear disagreement with the data. However, because of the partial cancellation between shear and bulk corrections, it is possible to increase both η and ζ simultaneously without changing $v_2(p_T)$ very much. This is demonstrated in Fig. 9, where we show that $v_2(p_T \lesssim 2\ \text{GeV})$ is fairly stable in the range $(\eta/s, \zeta/s) = (0.16, 0.005)$ to $(\eta/s, \zeta/s) = (0.4, 0.012)$.

This result does not imply that the data do not constrain η and ζ separately. In Fig. 10, we show the p_T-integrated flow parameter v_2 for pions and protons as a function of the number of participants. The number of participants was determined from the Glauber model used in [2]. We observe that p_T integrated v_2 is quite insensitive to the bulk viscosity. There are two reasons for this result. First, for values of ζ/s

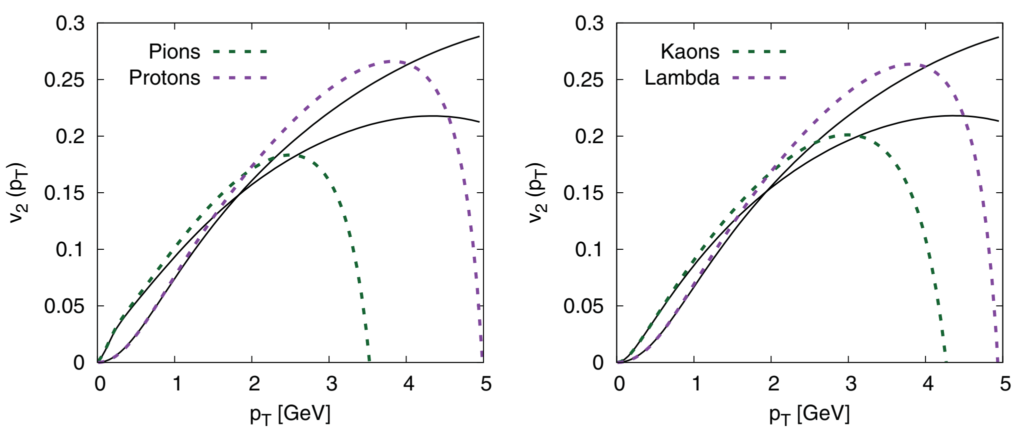

FIG. 8. (Color online) Differential elliptic flow $v_2(p_T)$ for pions and protons (left panel), as well as kaons and lambdas (right panel). The curves are labeled as in Fig. 6. The solid lines show the result for shear viscosity only, and the dashed lines correspond to shear and bulk viscosity with $\eta/s = 0.16$ and $\zeta/s = 0.005$.

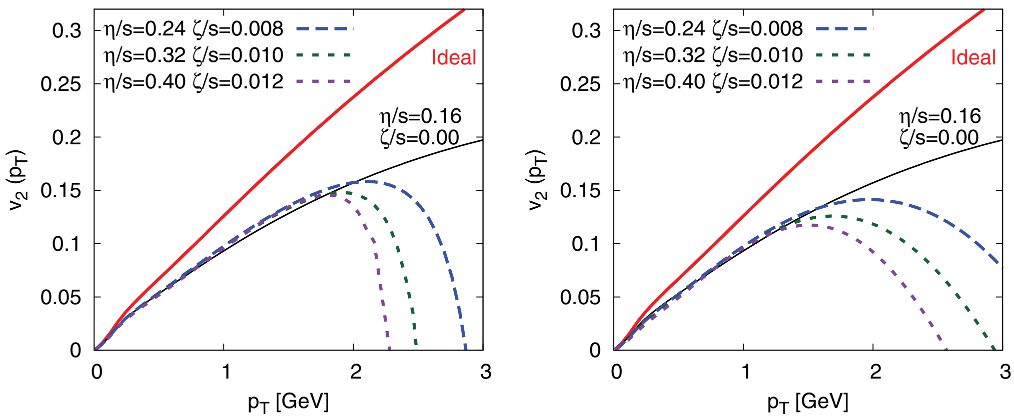

FIG. 9. (Color online) Differential elliptic flow of pions using the linearized expression for δf (left) and the resummed form of δf (right). The same $v_2(p_T)$ can be obtained for $p_T \lesssim 2$ GeV when increasing η/s by a factor of 2.5 as long as the bulk viscosity is increased as well.

in the range studied in this work, the effect of bulk viscosity on the velocity field is small. Larger values of ζ/s may lead to stronger effects on the integrated v_2. Second, because of Landau matching, the p_T-integrated change in the distribution function is small.

VII. SUMMARY AND OUTLOOK

In this work, we examined the functional form of the nonequilibrium correction to the particle phase-space distribution caused by bulk viscosity (see the summary in Fig. 11). In the high-temperature quark-gluon phase, the distribution function can be computed using the leading-log approximation. In this limit, bulk viscosity is controlled by $2 \leftrightarrow 2$ processes that rearrange momentum. Particle-number-changing $2 \leftrightarrow 3$ processes only play an indirect role, in that they prevent the development of an effective chemical potential for gluon or quark number.

We showed that there is a significant bulk viscous correction to the quark and gluon elliptic flow even for a fairly small bulk viscosity coefficient. In addition, there are nontrivial differences in the quark and gluon off-equilibrium distribution function. These differences are related to differences in the transport coefficients and effective masses. While the quark and gluon distributions are not directly observable, these distributions serve as direct input for calculations of photon and dilepton production from a bulk viscous medium. The effect of shear viscous corrections to the distribution function on photon and dilepton production was studied in [51–54]. It is conceivable that bulk viscosity is responsible for the large elliptic flow of photons as compared to hadrons that was recently observed by the PHENIX collaboration [55]. This possibility is related to the fact that the bulk strain is larger at early times, when most photons are produced, and to our observation that bulk viscosity enhances $v_2(p_T)$ at intermediate p_T.

For the hadron resonance stage near T_c, the calculation of the distribution functions is more difficult, and one has to rely on simplified models. The simplest model is the relaxation time approximation. The relaxation time approximation correctly captures the scaling of ζ and χ with the deviation from conformal symmetry, but it can not predict the functional form of $\chi(p)$ [it relates the behavior of $\chi(p)$ to the unknown energy dependence of τ], and it is in general not consistent with Landau matching. The relaxation time approximation

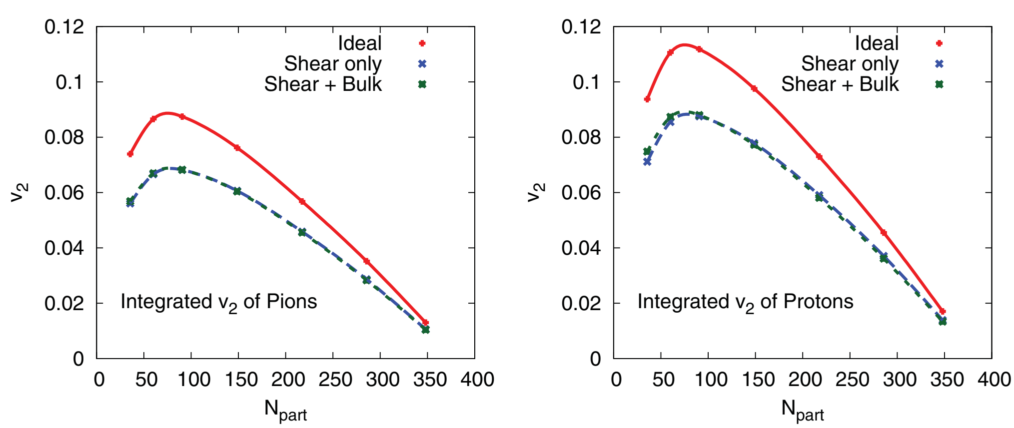

FIG. 10. (Color online) Integrated v_2 as a function of the number of participants for pions (left panel) and protons (right panel). We show the result in ideal hydrodynamics, the case of only shear viscosity with $\eta/s = 0.16$, and the case of both shear and bulk viscosity with $\eta/s = 0.16$ and $\zeta/s = 0.005$.

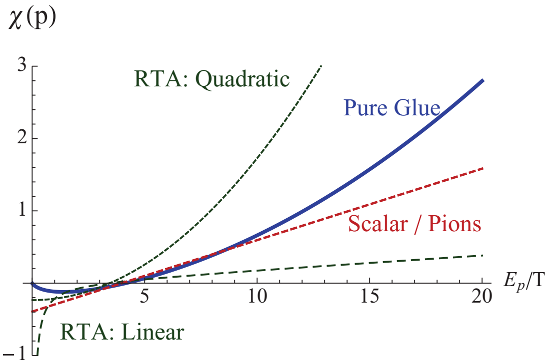

FIG. 11. (Color online) In this figure, we summarize different functional forms of the correction to the single-particle distribution function due to bulk viscosity $\chi_\Pi(p)$. The curves show the linear and quadratic form of the relaxation time approximation, the result in leading-log pure gauge theory, and the result in a gas of massive pions.

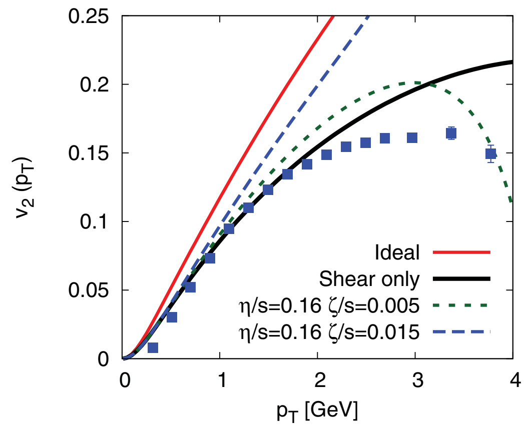

FIG. 12. (Color online) Elliptic flow of K_S mesons from viscous hydrodynamics. The hydrodynamic model was tuned such that the "shear only" result (solid black curve) fits the data points. The short-dashed green curve and long-dashed blue curve show results from viscous hydrodynamics having a bulk viscosity to entropy ratio $\zeta/s = 0.005$ and $= 0.015$, respectively. The data were obtained by the STAR collaboration at RHIC [56].

also assumes that shear and bulk viscosity are related to the same process, which need not be the case.

A simple model for theories in which bulk viscosity is controlled by chemical nonequilibration is scalar ϕ^4 theory. In this theory, the form of the nonequilibrium distribution functions is determined by the exact (energy) and approximate (particle-number) zero modes of the collision operator $\chi \simeq \chi_0 - \chi_1 E_{\mathbf{p}}$. The coefficient of χ_0 is related to the chemical equilibration time τ^{chem}, and χ_1 is fixed by Landau matching. For a given expansion rate $(\partial^k u_k) = 1/\tau$, we can also relate χ^0 to the effective chemical potential that describes the overpopulation of the single-particle distribution function $\mu \simeq -\frac{T}{\tau}\chi_0$.

The bulk viscosity and nonequilibrium distribution function in a low-temperature pion gas is correctly captured by the physics of scalar ϕ^4 theory with the appropriate chemical equilibration time. In this work, we assume that this is also true for a hadron resonance gas. We assume, in particular, that the nonequilibrium distribution function of the hadron species a is of the form $\chi^a \simeq \chi_0^a - \chi_1 E_{\mathbf{p}_a}$, where χ_1 is again fixed by Landau matching. The relative magnitude of the coefficient χ_0^a for different species was fixed by a simple model for the effective chemical potentials of meson and baryon resonances.

In an expanding system, inefficiencies in particle-number-changing processes lead to a particle excess, and both $\chi_0(\partial^k u_k)$ and $\chi_1 E_{\mathbf{p}}(\partial^k u_k)$ are negative. This means that bulk viscosity softens the p_T spectra of the produced particles. The change in the spectra leads to an enhancement of $v_2(p_T)$ at intermediate momenta $p_T \sim$ (1–2) GeV. This enhancement tends to cancel against the effects of shear viscosity. We showed, however, that the shear viscosity can be determined reliably by focusing on the p_T-integrated elliptic flow parameter. We also showed that bulk viscosity tends to preserve the approximate "quark-number scaling" observed in in the identified particle $v_2(p_T)$. Once η is fixed, bulk viscosity is strongly constrained by the spectra and $v_2(p_T)$. The main difficulty is that in the hadron resonance gas, the relationship between $\chi(p)$ and ζ is very sensitive to the contribution from high-lying resonances.

For the results shown in Figs. 6–10, we used $(\zeta/s)_{\text{frzout}} \lesssim 0.005$, and found modest bulk viscous correction to $v_2(p_T)$. In order to obtain a rough bound on the maximum value of ζ/s allowed by the data obtained at RHIC, we have studied the dependence of our results on ζ/s. Figure 12 shows the $v_2(p_T)$ for identified K_S mesons. We have chosen K_s mesons because the contribution from resonance decays, which were not included in this work, are negligible. Our hydrodynamic model was tuned previously to reproduce the measured spectra using shear viscosity only. This implies that the inclusion of bulk viscosity will typically worsen the agreement with data. For $(\zeta/s)_{\text{frzout}} = 0.005$, discrepancies with the data are not large, and the previous level of agreement could presumably be restored by retuning the parameters of the hydrodynamic model. For $(\zeta/s)_{\text{frzout}} \approx 0.015$, the discrepancy with data in the range $1 \lesssim p_T \lesssim 2$ GeV is significant, and it is unlikely that agreement with the data could be achieved without affecting other observables, such as the p_T integrated v_2. We therefore feel that it is safe to claim that the resonance gas model implies $(\zeta/s)_{\text{frzout}} \lesssim 0.015$. We plan to perform more detailed fits in the future.

The most important uncertainty in this bound is related to model dependence in the relation between $\chi(p)$ and ζ. In the hadron resonance gas, this relation depends on the inelastic cross sections of high-lying resonances. We can estimate the uncertainty of our results by reducing the number of resonances included in the model. For example, if we only keep mesons (baryons) with masses below 0.8 (1.0) GeV, we find $\chi_\pi^0 \simeq -30\zeta/(sT)$. This relation allows for roughly identical fits to the spectra with a ζ/s larger by about a factor of 3. We conclude that a more conservative bound is given by $(\zeta/s)_{\text{frzout}} \lesssim 0.05$. We emphasize that the data support a nonvanishing bulk viscosity. Statistical fits to hadronic yields [57] show the need to increase the abundance of baryons (i.e., protons + antiprotons) through a chemical-abundance factor[10] $\gamma_q \approx 1.6$ at RHIC energies. This result can be naturally accounted for in terms of a nonvanishing bulk viscosity.

There are a number of issues that we have not addressed in this work. Clearly, more work is needed to constrain the bulk viscosity of a hadron resonance gas. We have also not taken into account a possible increase in the bulk viscosity near T_c due to critical fluctuations [58,59]. If there is a rapid increase in the bulk viscosity near T_c, one also expects a rapid rise in the bulk relaxation time. Onuki [60] showed that the bulk relaxation time diverges near T_c more rapidly than the bulk viscosity. This implies that the system may free-stream through the transition region without significant effects on single-particle observables. Clearly, further study in this direction is necessary.

ACKNOWLEDGMENTS

K.D. would like to thank D. Fernandez-Fraile for useful discussions. This work was supported by the US Department of Energy Grant No. DE-FG02-03ER41260.

APPENDIX A: DETAILS OF THE HYDRODYNAMIC EVOLUTION

In this Appendix, we summarize some details of the hydrodynamic calculations that were used to compute the velocity and temperature profiles that determine the spectra of produced particles. We assume longitudinal boost invariance with initial conditions in the transverse plane taken from a Glauber model (see Appendix A in [29] for more details). For all noncentral collisions, we have used an impact parameter of $b = 6.8$ fm, and a decoupling temperature $T_{\rm frzout} = 150$ MeV.

We solve second-order hydrodynamic equations using a second-order fluid model developed by Grmela and Öttinger [26,27]. This model is quite similar to the theory of Israel and Stewart [24,25]. Grmela and Öttinger introduce a new dynamical tensor variable $c_{\mu\nu}$. We will see in the following that this variable is closely related to the velocity gradient tensor $\pi_{\mu\nu}$. In the local rest frame, the stress-energy tensor takes the form

$$T^{ij}_{\rm LRF} = p(\delta^{ij} - \alpha c^{ij}), \tag{A1}$$

where α is a small parameter, which will be shown to be related to the relaxation time. The tensor variable $c_{\mu\nu}$ is conveniently defined to have the property

$$c_{\mu\nu}u^\nu = u_\mu. \tag{A2}$$

We decompose $c_{\mu\nu}$ in terms of isotropic and traceless components $\bar{c}$ and $\mathring{c}$:

$$c_{\mu\nu} = -u_\mu u_\nu + \mathring{c}_{\mu\nu} + \bar{c}_{\mu\nu}, \tag{A3}$$

$$\bar{c}_{\mu\nu} = \tfrac{1}{3}\left(c^\lambda_\lambda - 1\right)(g_{\mu\nu} + u_\mu u_\nu). \tag{A4}$$

The equations of motion are dictated by conservation of energy and momentum $\partial_\mu T^{\mu\nu} = 0$ along with an evolution equation for the tensor variable $c_{\mu\nu}$:

$$u^\lambda(\partial_\lambda c_{\mu\nu} - \partial_\mu c_{\lambda\nu} - \partial_\nu c_{\mu\lambda}) = -\frac{1}{\tau_0}\bar{c}_{\mu\nu} - \frac{1}{\tau_2}\mathring{c}_{\mu\nu}. \tag{A5}$$

In the limit that the relaxation times (τ_0, τ_2) are very small, the evolution equation yields

$$c^{ij} = \tau_2\left(\partial_i u^j + \partial_j u^i - \tfrac{2}{3}\delta^{ij}\partial_k u^k\right) + \tfrac{2}{3}\tau_0\delta^{ij}\partial_k u^k. \tag{A6}$$

Substituting the above equation into $T^{ij}_{\rm LRF}$ and comparing the result to the Navier-Stokes equation, the bulk and shear viscosities can be identified as

$$\eta = \tau_2 p\alpha, \qquad \zeta = \tfrac{2}{3}\tau_0 p\alpha. \tag{A7}$$

In our work, we have taken the parameter $\alpha = 0.7$. These relaxation times are small enough so that the Navier-Stokes limit is approximately maintained near freeze-out. This is demonstrated in Fig. 13 where the bulk viscous stress Π is

[10]The abundance factor γ has to be distinguished from the fugacity $\lambda = e^{\mu/T}$, which enhances the abundance of particles while suppressing that of antiparticles.

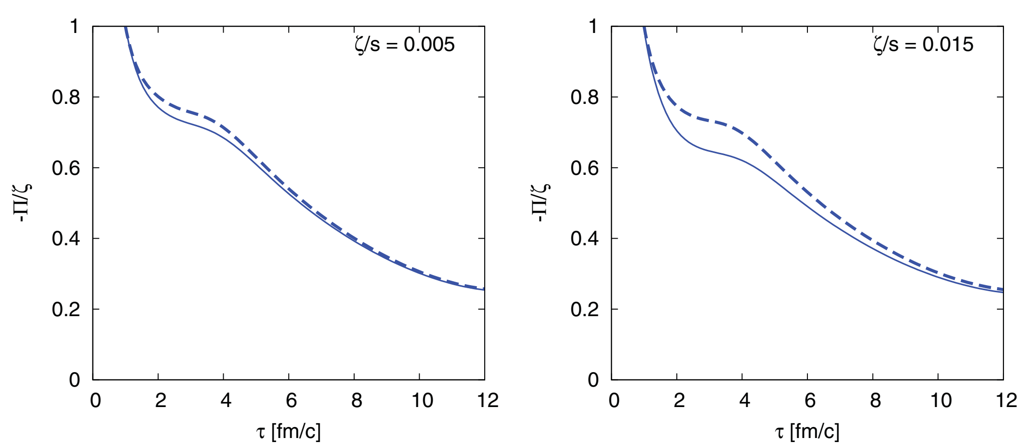

FIG. 13. (Color online) Bulk viscous pressure $-\Pi/\zeta$ (solid curves) versus proper time along the freeze-out hypersurface shown against the Navier-Stokes value $\partial_k u^k$ (dashed curve) for $(\zeta/s)_{\rm frzout} \approx 0.005$ (left) and $(\zeta/s)_{\rm frzout} \approx 0.015$ (right).

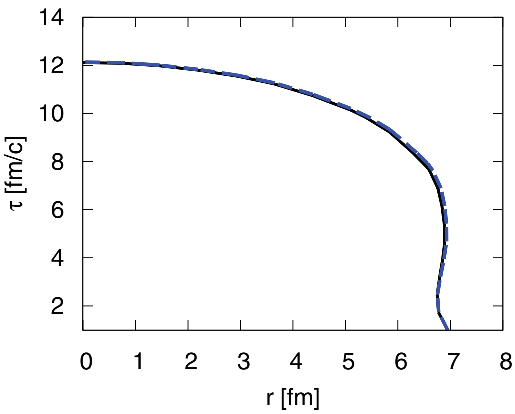

FIG. 14. (Color online) Freeze-out hypersurface ($T_{\rm frzout} = 150$ MeV) for a central ($b = 0$) collision with $\sigma_0 = 0.01$ [$(\zeta/s)_{\rm frzout} \approx 0.005$] shown as the solid black curve and for $\sigma_0 = 0.03$ [$(\zeta/s)_{\rm frzout} \approx 0.015$] shown as the dashed blue curve.

plotted versus the Navier-Stokes expectation for a central ($b = 0$) collision. For reference, we also show the corresponding freeze-out hypersurface in Fig. 14. The dynamical variable $c_{\mu\nu}$ was initialized to the Navier-Stokes value.

In Fig. 5, we show the elliptic flow of quark and gluons obtained in a simulation with a pure QGP equation of state. In order to allow for a speed of sound that is different from the conformal value $c_s^2 = 1/3$, we use a polytropic equation of state

$$\mathcal{P} = (\gamma - 1)\epsilon. \tag{A8}$$

The adiabatic index γ is chosen in order to fix a constant sound speed $c_s^2 = 0.2$ compatible with lattice parametrizations near T_c. The viscous correction to the distribution was computed with a Debye mass $m_D = 3.9T$ so that the QGP sound speed is $c_s^2 = 0.2$, consistent with the speed of sound used in the hydrodynamic evolution. We employed a simple parametrization of the solution of the Fokker-Planck equation for the off-equilibrium distribution functions. The parametrization is given in Table I.

All final-state hadron spectra shown in this work were calculated using a realistic equation of state, which is a parametrization of the lattice QCD equation of state from [8]. This equation of state matches to our hadron resonance gas equation of state below $T \sim 160$ MeV. The bulk viscosity during the hydrodynamic evolution was assumed to scale with

TABLE I. Parametrization of the leading-log QCD off-equilibrium distribution function. We use the functional form $\chi_\Pi(p) = (c_0 p^{x_0} + c_1 p^{x_1}) \ln(p/p_0)$, for $m_D = 3.9$ and $N_f = 2$. The above parametrization yields $\zeta/T^3 \approx 3.07$.

	Quarks	Gluons
p_0	2.51	4.32
c_0	9.56×10^{-2}	6.28×10^{-2}
x_0	5.25×10^{-1}	9.56×10^{-1}
c_1	8.64×10^{-3}	3.43×10^{-6}
x_1	1.66	3.48

the second power of conformality breaking

$$\zeta/s = 15\sigma_0\left(\tfrac{1}{3} - c_s^2\right)^2, \tag{A9}$$

where σ_0 is a free parameter chosen to set the desired magnitude of the bulk viscosity coefficient near freeze-out. At our freeze-out temperature of 150 MeV, the lattice equation of state used in this work yields $c_s^2 \approx 0.15$. In Sec. VI B, we examine a hadronic resonance gas with $(\zeta/s)_{\rm frzout} \approx 0.005$, corresponding to $\sigma_0 = 0.01$.

APPENDIX B: PHASE SPACE INTEGRALS

1. Relaxation time approximation

In the relaxation time approximation, we found the relationship between the shear viscosity and energy-dependent relaxation time $\tau_R(E_{\mathbf{p}})$ in Eq. (32), which we rewrite here as

$$\eta = \frac{\beta}{30\pi^2} \int \frac{p^6}{E_{\mathbf{p}}^2} \tau_R(E_{\mathbf{p}}) n_{\mathbf{p}}(1 \pm n_{\mathbf{p}})\, dp. \tag{B1}$$

If we take a relaxation time of the form

$$\tau_R(E_{\mathbf{p}}) = \tau_0 \beta (\beta E_{\mathbf{p}})^{1-\alpha}, \tag{B2}$$

the relationship becomes

$$\eta = \tau_0 \frac{\beta^4}{30\pi^2} \int \frac{p^6}{(\beta E_{\mathbf{p}})^{1+\alpha}} n_{\mathbf{p}}(1 \pm n_{\mathbf{p}})\, dp. \tag{B3}$$

Making the change of variables $x \equiv \beta E_{\mathbf{p}}$, we find Eq. (34):

$$\eta = \tau_0 \frac{T^3}{30\pi^2} \mathcal{I}_\alpha(\beta m), \tag{B4}$$

where the remaining phase-space integral is

$$\mathcal{I}_\alpha(\beta m) \equiv \int_{\beta m}^{\infty} \frac{[x^2 - (\beta m)^2]^{5/2}}{x^\alpha} n_{\mathbf{x}}(1 \pm n_{\mathbf{x}}) dx. \tag{B5}$$

Even though we have arrived at the above phase-space integral by studying the relaxation time approximation, it will turn out we will need the same phase-space integrals in other contexts as well. It is therefore worthwhile to study some limits where analytic results can be obtained. For a classical gas, we can replace $n_{\mathbf{x}}(1 \pm n_{\mathbf{x}}) \to n_{\mathbf{x}}$ and the phase-space integral can be computed analytically when $\alpha = 0$:

$$\mathcal{I}_{\alpha=0} = 15(\beta m)^3 K_3(\beta m). \tag{B6}$$

Another case where an analytic expression can be found is in the high-temperature limit ($\beta m \to 0$). For $\alpha < 4$, we find

$$\mathcal{I}_\alpha(\beta m = 0) = \overline{\Gamma}(6 - \alpha), \tag{B7}$$

where for convenience we have defined[11]

$$\overline{\Gamma}(x) \equiv \begin{cases} \Gamma(x) & \text{Maxwell}, \\ \Gamma(x)\zeta_+(x-1) & \text{Bose}, \\ \Gamma(x)\zeta_-(x-1) & \text{Fermi} \end{cases} \tag{B9}$$

for $x > 2$ and where

$$\zeta_\pm(s) \equiv \sum_{k=1}^{\infty} \frac{(\pm)^{k-1}}{k^s}. \tag{B10}$$

$\zeta_+(s)$ is the usual Riemann-zeta function and $\zeta_-(s) = (1 - 2^{1-s})\zeta_+(s)$. We will also need the $\alpha = 4$ behavior of the above phase-space integral. For classical and Fermi statistics, the above results hold as long as we note that $\lim_{s\to 1} \zeta_-(x) = \ln 2$. We therefore have that $\mathcal{I}_{\alpha=4} = \Gamma(2)$ for classical statistics and $\mathcal{I}_{\alpha=4} = \Gamma(2)\ln(2)$ for Fermi statistics. The above integral is logarithmically divergent for bosons when $\alpha = 4$. The divergence is regulated by the mass (or thermal mass) of the relevant quasiparticles. We define the following values for $\overline{\Gamma}(x = 2)$:

$$\overline{\Gamma}(x=2) \equiv \begin{cases} \Gamma(2) & \text{Maxwell}, \\ \ln\left(\frac{2T}{m}\right) - \frac{8}{15} & \text{Bose}, \\ \Gamma(2)\ln(2) & \text{Fermi}. \end{cases} \tag{B11}$$

The relevant phase-space integral for bulk viscosity can be found by using the change of variable $x \equiv \beta E_{\mathbf{p}}$ in Eqs. (35) and (36):

$$\mathcal{J}_\alpha(\beta m, \beta\tilde{m}) \equiv \int_{\beta m}^{\infty} \frac{[x^2 - (\beta m)^2]^{5/2}}{x^\alpha} n_{\mathbf{x}}(1 \pm n_{\mathbf{x}}) \times \left[\frac{1}{3} - c_s^2\left(1 + \frac{(\beta\tilde{m})^2}{x^2 - (\beta m)^2}\right)\right]^2 dx. \tag{B12}$$

As in the shear case, analytic expressions are available. For $\alpha = 0$ and classical statistics, we find

$$\begin{aligned}\mathcal{J}_{\alpha=0} = {} & 15\left(\tfrac{1}{3} - c_s^2\right)^2 (\beta m)^3 K_3(\beta m) \\ & - 6(\beta\tilde{m}c_s)^2\left(\tfrac{1}{3} - c_s^2\right)(\beta m)^2 K_2(\beta m) \\ & + (\beta\tilde{m}c_s)^4 (\beta m) K_1(\beta m).\end{aligned} \tag{B13}$$

If both βm and $\beta\tilde{m}$ are taken to zero, the integral is

$$\mathcal{J}_\alpha = \left(\tfrac{1}{3} - c_s^2\right)^2 \overline{\Gamma}(6-\alpha). \tag{B14}$$

Another limit of interest is when $(\beta m) \to 0$ but $\tilde{m}$ remains finite. This is physically relevant since $\tilde{m}$ quantifies the deviations from conformality, which is crucial to keep when studying bulk viscosity, while the bare or thermal mass only effects the kinematics in the phase-space integrals. The only subtlety is if the phase-space integral is logarithmically divergent, in which case the mass serves as a cutoff for the integral. The resulting expression in this limit is

$$\begin{aligned}\mathcal{J}_\alpha = {} & \left(\tfrac{1}{3} - c_s^2\right)^2 \overline{\Gamma}(6-\alpha) - 2(\beta\tilde{m}c_s)^2\left(\tfrac{1}{3} - c_s^2\right)\overline{\Gamma}(4-\alpha) \\ & + (\beta\tilde{m}c_s)^4\, \overline{\Gamma}(2-\alpha).\end{aligned} \tag{B15}$$

2. Scalar field theory

In this section, we evaluate the necessary phase-space integrals for a scalar field theory. Let us first start with the integral labeled $\mathcal{F}$ in Eq. (60):

$$\mathcal{F} = \int \frac{d^3\mathbf{p}}{(2\pi)^3 E_{\mathbf{p}}} \left(\frac{p^2}{3} - c_s^2 E_{\mathbf{p}} \frac{\partial(\beta E_{\mathbf{p}})}{\partial\beta}\right) n_{\mathbf{p}}(1 + n_{\mathbf{p}}). \tag{B16}$$

In the high-temperature limit, we can take $\beta m \to 0$ while keeping $\tilde{m}$ finite. Using the phase-space integrals defined in Appendix B1, we find[12]

$$\tilde{\Gamma}(x=2) \equiv \lim_{m\to 0} \beta^2 \int \frac{\mathbf{p}^2}{E_{\mathbf{p}}} n_{\mathbf{p}}(1 \pm n_{\mathbf{p}}) dp = \begin{cases} \Gamma(2) & \text{Maxwell}, \\ \ln\left(\frac{2T}{m}\right) & \text{Bose}, \\ \Gamma(2)\ln(2) & \text{Fermi}, \end{cases} \tag{B17}$$

$$\mathcal{F} = \frac{T^4}{2\pi^2}\left[\left(\frac{1}{3} - c_s^2\right)\overline{\Gamma}(4) - (\tilde{m}\beta)^2 c_s^2 \tilde{\Gamma}(2)\right]. \tag{B18}$$

The function $\mathcal{F}$ characterizes the deviation from conformality. The relationship between the shifted mass $\tilde{m}$ and the sound speed can be found by using the fact that the source term for bulk viscosity is orthogonal to the energy-changing zero mode

$$0 = \int \frac{d^3\mathbf{p}}{(2\pi)^3} n_{\mathbf{p}}(1 \pm n_{\mathbf{p}}) \left(\frac{\mathbf{p}^2}{3} - c_s^2 \tilde{E}_{\mathbf{p}}^2\right). \tag{B19}$$

This leads to

$$\tfrac{1}{3} - c_s^2 \approx (\tilde{m}\beta)^2 \tfrac{\overline{\Gamma}(3)}{3\overline{\Gamma}(5)}. \tag{B20}$$

Using this relation, we find for bosons

$$\mathcal{F} = \frac{(\tilde{m}T)^2}{6\pi^2}\left[\frac{15\zeta_+(3)}{2\pi^2} - \ln\left(\frac{2T}{m}\right)\right]. \tag{B21}$$

[11]We have used the relation

$$\int_0^\infty \frac{x^{n-1}}{e^x \mp 1} dx = \zeta_\pm(n)\Gamma(n), \tag{B8}$$

which can be derived by expanding the numerator in terms of its geometric series and then performing the integral of each term in the series individually. The remaining summation will then be of the form (B10).

[12]In Appendix B1, the phase-space integral in Eq. (B3) has the form $\int \mathbf{p}^6/E_{\mathbf{p}}^{1+\alpha}$. The term in Eq. (B16) proportional to $\tilde{m}^2$ has the form $\int \mathbf{p}^{6-\alpha}/E_{\mathbf{p}}$. For massless particles, these two integrals are the same except if $\alpha = 4$ in the case of bosons. This is due to the way the logarithmic divergence is regulated in the two cases. In the latter case, where there is only one power of $E_{\mathbf{p}}$ in the denominator we define Eq. (B17).

[1] S. S. Adler *et al.*, Phys. Rev. Lett. **91**, 182301 (2003).
[2] K. Dusling and D. Teaney, Phys. Rev. C **77**, 034905 (2008).
[3] Paul Romatschke and Ulrike Romatschke, Phys. Rev. Lett. **99**, 172301 (2007).
[4] Huichao Song, and Ulrich W. Heinz, Phys. Rev. C **77**, 064901 (2008).
[5] Thomas Schäfer and Derek Teaney, Rep. Prog. Phys. **72**, 126001 (2009).
[6] P. K. Kovtun, D. T. Son, and A. O. Starinets, Phys. Rev. Lett. **94**, 111601 (2005).
[7] Huichao Song, Steffen A. Bass, Ulrich Heinz, Tetsufumi Hirano, and Chun Shen, Phys. Rev. Lett. **106**, 192301 (2011).
[8] Mikko Laine and York Schroder, Phys. Rev. D **73**, 085009 (2006).
[9] Pasi Huovinen and Pter Petreczky, Nucl. Phys. A **837**, 26 (2010).
[10] P. Danielewicz and M. Gyulassy, Phys. Rev. D **31**, 53 (1985).
[11] Peter Brockway Arnold, Caglar Dogan, and Guy D. Moore, Phys. Rev. D **74**, 085021 (2006).
[12] Steven Weinberg, Astrophys. J. **168**, 175 (1971).
[13] Alex Buchel, Phys. Lett. B **663**, 286 (2008).
[14] A. Bazavov, T. Bhattacharya, M. Cheng, N. H. Christ, C. DeTar *et al.*, Phys. Rev. D **80**, 014504 (2009).
[15] Harvey B. Meyer, Phys. Rev. Lett. **100**, 162001 (2008).
[16] G. S. Denicol, T. Kodama, T. Koide, and Ph. Mota, Phys. Rev. C **80**, 064901 (2009).
[17] Akihiko Monnai and Tetsufumi Hirano, Phys. Rev. C **80**, 054906 (2009).
[18] Huichao Song and Ulrich W. Heinz, Phys. Rev. C **81**, 024905 (2010).
[19] Piotr Bozek, Phys. Rev. C **81**, 034909 (2010).
[20] Piotr Bozek (unpublished).
[21] Piotr Bozek, Phys. Lett. B **699**, 283 (2011).
[22] G. S. Denicol, T. Kodama, and T. Koide, J. Phys. G: Nucl. Part. Phys. **37**, 094040 (2010).
[23] Victor Roy and A. K. Chaudhuri, Phys. Lett. B **703**, 313 (2011).
[24] W. Israel, Ann. Phys. (NY) **100**, 310 (1976).
[25] W. Israel and J. M. Stewart, Ann. Phys. (NY) **118**, 341 (1979).
[26] Miroslav Grmela and Hans Christian Ottinger, Phys. Rev. E **56**, 6620 (1997).
[27] Hans Christian Ottinger, Phys. Rev. E **57**, 1416 (1998).
[28] Fred Cooper and Graham Frye, Phys. Rev. D **10**, 186 (1974).
[29] Kevin Dusling, Guy D. Moore, and Derek Teaney, Phys. Rev. C **81**, 034907 (2010).
[30] John E. Davis and Robert J. Perry, Phys. Rev. C **43**, 1893 (1991).
[31] P. Chakraborty and J. I. Kapusta, Phys. Rev. C **83**, 014906 (2011).
[32] Jiunn-Wei Chen, Jian Deng, Hui Dong, and Qun Wang (unpublished).
[33] M. Bluhm, B. Kampfer, and K. Redlich, Phys. Rev. C **84**, 025201 (2011).
[34] Sangyong Jeon, Phys. Rev. D **52**, 3591 (1995).
[35] Sangyong Jeon and Laurence G. Yaffe, Phys. Rev. D **53**, 5799 (1996).
[36] Steven Weinberg, *Cosmology* (Oxford University Press, Oxford, UK, 2008), p. 593.
[37] Egang Lu and Guy D. Moore, Phys. Rev. C **83**, 044901 (2011).
[38] Juhee Hong and Derek Teaney, Phys. Rev. C **82**, 044908 (2010).
[39] Peter Brockway Arnold, Guy D. Moore, and Laurence G. Yaffe, J. High Energy Phys. **0011**, 001 (2000).
[40] Peter Brockway Arnold, Guy D. Moore, and Laurence G. Yaffe, J. High Energy Phys. **0301**, 030 (2003).
[41] Jiunn-Wei Chen and Juven Wang, Phys. Rev. C **79**, 044913 (2009).
[42] D. Fernandez-Fraile and A. Gomez Nicola, Phys. Rev. Lett. **102**, 121601 (2009).
[43] Antonio Dobado, Felipe J. Llanes-Estrada, and Juan M. Torres-Rincon, Phys. Lett. B **702**, 43 (2011).
[44] S. Pratt and K. Haglin, Phys. Rev. C **59**, 3304 (1999).
[45] J. L. Goity, Phys. Lett. B **319**, 401 (1993).
[46] Chungsik Song and Volker Koch, Phys. Rev. C **55**, 3026 (1997).
[47] E. L. Bratkovskaya, W. Cassing, C. Greiner, M. Effenberger, U. Mosel *et al.*, Nucl. Phys. A **675**, 661 (2000).
[48] J. Noronha-Hostler, C. Greiner, and I. A. Shovkovy, Phys. Rev. Lett. **100**, 252301 (2008).
[49] Ralf Rapp and Edward V. Shuryak, Phys. Rev. Lett. **86**, 2980 (2001).
[50] R. Rapp, Phys. Rev. C **63**, 054907 (2001).
[51] Kevin Dusling and Shu Lin, Nucl. Phys. A **809**, 246 (2008).
[52] Kevin Dusling, Nucl. Phys. A **839**, 70 (2010).
[53] Jitesh R. Bhatt, Hiranmaya Mishra, and V. Sreekanth, J. High Energy Phys. **1011**, 106 (2010).
[54] Maxime Dion, Charles Gale, Sangyong Jeon, Jean-Francois Paquet, Bjoern Schenke *et al.*, J. Phys. G: Nucl. Part. Phys. **38**, 124138 (2011).
[55] A. Adare *et al.* (unpublished).
[56] B. I. Abelev *et al.*, Phys. Rev. C **77**, 054901 (2008).
[57] Jean Letessier and Johann Rafelski, Eur. Phys. J. A **35**, 221 (2008).
[58] Dmitri Kharzeev and Kirill Tuchin, J. High Energy Phys. **0809**, 093 (2008).
[59] Guy D. Moore and Omid Saremi, J. High Energy Phys. **0809**, 015 (2008).
[60] Akira Onuki, Phys. Rev. E **55**, 403 (1997).